Spring 1-1-2021

Holomorphic Embedded Load-flow Method's Application on Three-phase Distribution System With Unbalanced Wyeconnected Loads

Nitin Gupta
Cleveland State University

HOLOMORPHIC EMBEDDED LOAD-FLOW METHOD'S APPLICATION ON THREE-PHASE DISTRIBUTION SYSTEM WITH UNBALANCED WYE-CONNECTED LOADS

NITIN GUPTA

Bachelor's Degree Received

Bharati Vidyapeeth's College of Engineering

June 2016

Submitted in partial fulfillment of requirements for the degree

MASTER OF SCIENCE IN ELECTRICAL ENGINEERING

at the

CLEVELAND STATE UNIVERSITY

May 2021

We hereby approve this thesis for

NITIN GUPTA

Candidate for the Master's in electrical engineering degree for the

Department of Electrical Engineering and Computer Science

and the

CLEVELAND STATE UNIVERSITY'S

College of Graduate Studies by

Committee Chairperson, Dr Hongxing Ye

Dept. of Electrical Eng. and Computer Science & April 29, 2021

Committee Member, Dr Hongkai Yu

Dept. of Electrical Eng. and Computer Science & April 29, 2021

Committee Member, Dr Zhiqiang Gao

Dept. of Electrical Eng. and Computer Science & April 29, 2021

Student's Date of Defense: April 29, 2021

ACKNOWLEDGMENT

I would like to sincerely thank my supervisor, Dr. Hongxing Ye, for his guidance during my thesis research. He has always been available to kindly answer my questions and provide comments about my work. He has also helped me to give shape to my research and to stay always motivated. I want to thank the members of the thesis committee, Dr Hongkai Yu and Dr Zhiqiang Gao, for their assessment of my work. I would also like to thank my lab mate, Shubo Zhang and close friends for all their help. I want to acknowledge the support from the Cleveland State University. Finally, I want to express my greatest gratitude to my entire family for their support and patience.

HOLOMORPHIC EMBEDDED LOAD FLOW METHOD'S APPLICATION ON THREE-PHASE DISTRIBUTION SYSTEM WITH UNBALANCED WYE-CONNECTED LOADS

NITIN GUPTA

ABSTRACT

With increasing load and aging grid infrastructure, an accurate study of power flow is very important for operation and planning studies. The study involves a numerical calculation of unknown parameters, such as voltage magnitude, angle, net complex power injection at buses and power flow on branches. The performance of traditional iterative power flow methods, such as Newton-Raphson, depends on initial starting point, does not guarantee solution for heavily loaded, and poor convergence for unbalanced radial power system.

Holomorphic load embedding is a non-iterative and deterministic method for finding steady-state solutions of any power system network. The method involves converting voltage parameter at every bus into an embedded parameter (α) where analytic continuation is applied using Pade` approximants. The embedded parameter (α) acts as a well-defined reference for the complex analysis and solution obtained when setting a simple value α is known as Germ Solution, by some texts. Using the values of coefficient of Maclaurin Series, the Holomorphic method can find solutions in the whole complex plane using analytic continuation as it extends the nature of function beyond the radius of convergence.

The holomorphic embedding method has been applied in the past to solve power flow problems in balanced power system models. There are several advantages of the

said method over traditional iterative techniques, such as guaranteed convergence, the existence of solution, and faster calculation for certain cases. The method dives into complex analysis, algebraic curves, Taylor series expansion, Pade` approximants, and solving a linear set of equations.

. For simplicity purpose, the networks are often assumed to be balanced with constant power loads. Power flow analysis and its derivatives are performed on a single-phase equivalent of the same system. For bulk systems, the assumption is acceptable as load aggregation balances the loads in each phase to an acceptable level. However, in low-voltage distribution systems, ignoring such parameter could lead to an incorrect solution. In this work, a class of Holomorphic load-flow method is proposed to solve the power flow problem in three-phase distribution systems with unbalanced wye-connected loads.

Keywords – *Three-phase Distribution system, Holomorphic load-flow Embedding, Analytic Continuation, and non-iterative.*

TABLE OF CONTENTS

Page

LIST OF TABLES

Table Page

LIST OF FIGURES

Figure Page

LIST OF NOMENCLATURE

i, k	i^{th}, k^{th} Bus/Node in the Network
α	Holomorphic Embedding Parameter
$(.)^*$	Represents Complex Conjugate of a Term
$(.)^T$	Represents Transpose of a vector
n_b	Number of Buses or Laterals in the System
n_g	Number of Generating Units in the System
PQ	Set of Load Buses in the system
PV	Set of Generation Buses in the system
N	Number of Total Buses, Nodes in a Network
HELM	Holomorphic Embedded Load-flow Method
CPF	Continuation Power Flow
PBE	Power Balance Equations
ROC	Region of Convergence
RHS	Right-hand side of an equation
S_i	Complex Power Injection at Bus i
P_i	Net Real/active power injection at Bus i
Q_i	Net Reactive power injection at Bus i
V_{source}	Voltage at the Substation Transformer in Radial Distribution System
V_{slack}	Slack Bus Voltage in the Network, typically set to 1.0 Per Unit
V	Per Unit Voltage Vector for Each Bus ($N \times 1$ Dimensions)
I	Per Unit Current Vector for Each Bus ($N \times 1$ Dimensions)

V_i	Per Unit Voltage at bus *i*
I_i	Per Unit value of Current at Bus *i*
$\|V_i\|$	Voltage Magnitude at Bus *i*
δ_i	Voltage Angle in Radians at Bus *i*
$V_i(\alpha)$	Voltage at i^{th} Bus as a Function of Holomorphic Parameter α
$V_i[n]$	n^{th} Coefficient of Maclaurin Series of Voltage at i^{th} Bus
$V_{i,re[n]}$	Real Part of n^{th} Coefficient of Maclaurin Series of Voltage at i^{th} PV Bus
$V_i^{re}[n]$	Real Component of Voltage Coefficient $V_i[n]$
$V_i^{im}[n]$	Imaginary Component of Voltage Coefficient $V_i[n]$
$V_{sp,i}$	Voltage Set Point for i^{th} Bus
Y	Bus Admittance Matrix for the Network
Y^{trans}	Series Branch Part of Y Matrix
Y^{shunt}	Shunt Branch Part of Y Matrix
Y_{sym}^{trans}	Symmetric Submatrix of Y^{trans} Matrix
Y_{unsym}^{trans}	Unsymmetric Submatrix of Y^{trans} Matrix
τ	Tap changing transformer ratio with phase shift angle, $(\|\tau\|\angle\theta_{shift}^{\circ})$
$Y_{i,k}$	i^{th} row and k^{th} column element of Bus Admittance Matrix Y
$\theta_{i,k}$	Polar angle of i^{th} row and k^{th} column element of Y
R	Resistance in Ohms
X	Reactance in Ohms
P_l^{max}	Active Power flow Limit for Branch *l*
$abcn$	Represents phase-to-neutral quantities an, bn and cn.

V_i^{abc} Line to Line Three-Phase Voltage vector $\begin{bmatrix} V_{ab} \\ V_{bc} \\ V_{ca} \end{bmatrix}$ for i^{th} Bus

V_i^{abcn} Phase-to-neutral Three-Phase Voltage vector $\begin{bmatrix} V_a \\ V_b \\ V_c \end{bmatrix}$ for i^{th} Bus

$V_i^{abcn,0}$ Phase-to-neutral Germ solution Voltage vector $\begin{bmatrix} 1\angle 0° \\ 1\angle 120° \\ 1\angle -120° \end{bmatrix}$ for i^{th} Bus

V_i^{nom} Phase-to-neutral Three-Phase Nominal Voltage $\begin{bmatrix} V_a \\ V_b \\ V_c \end{bmatrix}$ for i^{th} Bus

I_i^{abc} Line to Line Three-Phase Current vector $\begin{bmatrix} I_{ab} \\ I_{bc} \\ I_{ca} \end{bmatrix}$ for i^{th} Bus

I_i^{abcn} Phase-to-neutral Three-Phase Current vector $\begin{bmatrix} I_a \\ I_b \\ I_c \end{bmatrix}$ for i^{th} Bus

$Z_{i,j}^{abc}$ Represents Phase-Frame Impedance Matrix for a Three-Phase Transmission Line between bus i and j

$Y_{i,j}^{abc}$ Represents Phase-Frame Admittance Matrix for a Three-Phase Transmission Line between bus i and j

CHAPTER I

INTRODUCTION

1.1 Power-flow Methods & their Problems

Power-flow or load-flow analysis is crucial for any power system, not only from the standpoint of operation and control, but also from protection, resilience, future planning [1]. The result of any Power-flow analysis is to obtaining steady-state parameters, such as voltage magnitude, $|V|$, and voltage angle, θ, on each bus, and other parameters, such as transmission line flow, active and reactive power components, could be derived from $|V|$ and θ. For a complete study of a power system, four parameters for each bus are required for each steady-state scenario, voltage magnitude, voltage angle, net active power injection and net reactive power injection. For each type of bus, two of the parameters are known and the other two are unknown, the details can be noted in Table 1.1 below.

Table 1 - Bus Types with Known and Unknown Parameter Details

Bus Type	Known Parameters	Unknown Parameters
Slack Bus or Reference Bus	$\|V\|$, θ	P, Q
PV Bus (Generator Bus)	P, $\|V\|$	Q, θ
PQ Bus (Load Bus)	P, Q	$\|V\|$, θ

The known parameters or variable in power-flow are network data (topology, branch impedances, shunt admittances, complex power generation limits for generators, etc.), net complex power injection at each load bus (also called as PQ bus), voltage and active power injection at each generator bus (also called as PV bus), and selection of slack bus in the network. Using the above-mentioned known parameter for a network, a power-flow study provides unknown parameters for each bus that can be obtained. The next aim is to derive branch flows, with all this information calculated about a power system, operators monitor and take actions to ensure that voltage, V, at each bus is with limits, and branch flow is under thermal limits, P_l^{max}. To solve any violations, power system operators in real-time can take actions, such as control complex power injection at desired buses to adjust $|V|\ and\ \theta$, which in turn can resolve any branch-flow violations.

The Alternating-Current power-flow analysis is non-linear due to the relation voltage square and complex power injection at each bus. The non-linear set of equations are traditionally solved using iterative methods which can be computationally intensive, if not NP-hard problems [2]. For large AC power system, Direct current (DC) approximation method is used which are fast to calculate and provides acceptable accuracy for operations [3].

Many variants of Iterative methods can be used to solve a power-flow problem that is numerically represented by a non-linear system of equations. Iterative methods, such as Gauss-Seidel (GS) method, Newton-Raphson (NR) method and its derivates such as the Fast-decoupled Newton-Raphson method is widely used in the industry. However, each method has benefits and shortcomings, GS method takes less memory, but is very

slow for larger networks, NR method calculates reliable solution only for scenarios when the system is operating at flat voltage.

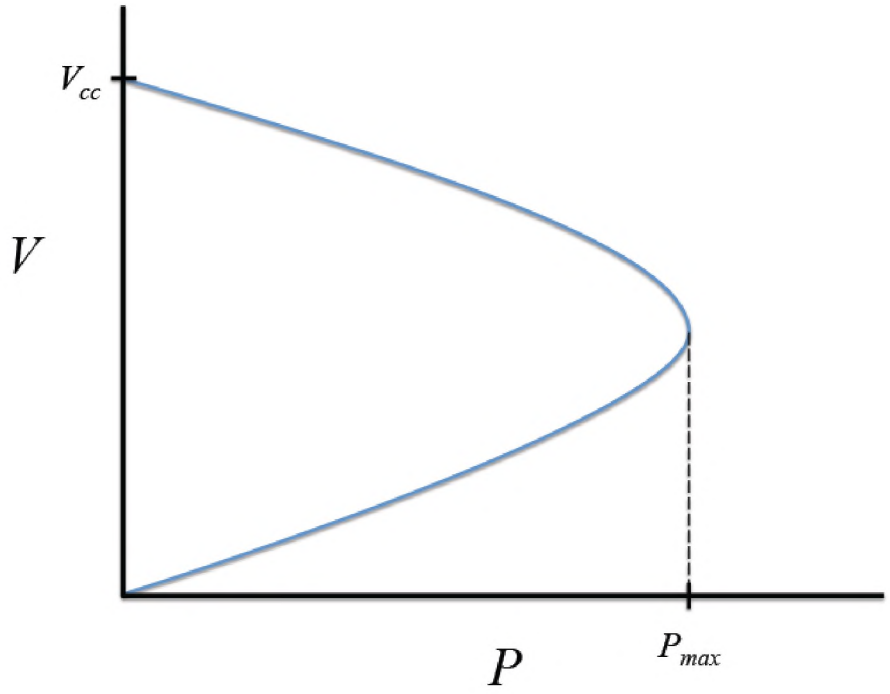

Figure 1 – PV curve which shows two solution branches and voltage bifurcation/collapse point

Iterative methods often have two major drawbacks. First, there is no guarantee of convergence after all iterations, and the convergence depends on the starting point of iterations which is reasoned from the fractal property of the solution plane. Second, there is no complete control over the choice of solution due to multiple solutions of a non-linear system of equations [2]. For the practical operation of the power system, a higher voltage solution is feasible which is close to a flat voltage profile, typically within 5% percent of 1.0 per unit [1]. Figure 1 shows the two solution branches, one low voltage

branch and one high voltage branch. For system stability reasons, a high voltage branch solution is desired for operation [4].

1.2 Basic of Holomorphic Embedding Method

After discussing the advantages and disadvantages of iterative methods in the previous section, in this section, non-iterative methods are discussed, specifically the holomorphic embedding load-flow method (HELM). It is known that closed-form solution to non-linear equation produces fast and accurate results [4]. However, finding a closed-form solution for a larger system with a different scenario is computationally very hard with present technology [5]. In the holomorphic embedding method, original power balance equations (PBE's), stated below, is embedded with a holomorphic parameter α, which transform the original PBEs into their analytical form. From the mathematical standpoint, analytical continuation is a complex analysis method used to expand the holomorphic function beyond the radius of convergence (given that function satisfy Cauchy-Reimann equations [6]) and thus extending the power series domain. In the below PBEs, N is the number of buses, $G_{i,k}$ and $B_{i,k}$ are real and imaginary part of the (i^{th}, k^{th}) element of the bus admittance matrix Y, respectively.

$$P_i = \sum_{k=1}^{N} |V_i||V_k|\left(G_{i,k}cos\theta_{i,k} + B_{i,k}sin\,\theta_{i,k}\right) \quad 1.1$$

$$Q_i = \sum_{k=1}^{N} |V_i||V_k|\left(G_{i,k}sin\theta_{i,k} - B_{i,k}cos\,\theta_{i,k}\right) \quad 1.2$$

The holomorphic embedding method always reaches the high-voltage operating point when the solution exists. In the meantime, it gives a clear indication if no solution exists.

1.3 Introduction to Three-Phase Distribution System

In the last few decades, the Distribution Systems (DS) have changed due to increasing load, distributed energy resources (DRE), and other factors. It is more important to accurately study power flow in DS due to reasons such as:

- Optimization and efficient use of distribution systems require answering questions like maximum operating capacity of feeders and other types of equipment.
- Need to modernize distribution systems with features such as smart metering and faster fault detection.
- Penetration of distributed energy resources, such as roof-top photovoltaic panels and electric vehicles acting as battery banks.
- Most faults occur on the distribution system of the power system and an accurate power flow study would improve resilience and reliability.

Analysis and optimization of the Distribution System end of the power system has been ignored for a long time due to technical difficulties [7]. With the introduction of micro-Renewable Energy Source (RES), accurate power-flow analysis of distribution systems has become more important. General iterative methods produce inaccurate results for DS, the problems mentioned below in points are the reason for that.

- Loads on radial single-phase distribution feeders are unbalanced in comparison to the other phases.

- Additionally, overhead or underground conductor configuration of the three-phases lines introduces mutual inductance between the phases.
- At a lower voltage of DS, resistive losses cannot be ignored as they are significant. Therefore, resistance in branches is taken into network parameters.
- For better modeling of DS, taking into account of the type of load is necessary. Modeling of constant impedance, current, and power loads (collectively known as ZIP loads) will further improve the accuracy of the analysis.
- Other parameters such as configurations of lines on poles, transposition of conductors, and transformer connection cause inaccuracy in traditional power-flow methods.

The methods mentioned in Section 1.1 are generally applied to high-voltage, single-phase equivalent of a balanced system. However, towards the lower voltage side of the power system, i.e., the Distribution System (DS), is inherently unbalanced due to unpredictable consumption of power on each phase or lateral. Factors such as transmission line spacing configurations, conductor type, the resistance of the conductor and the possibility of no load on some phases, etc., play an important role in power flow solution [7]. Approximate methods such as voltage drop over a radial network and ladder-iterative methods provide approximate solutions [8]. For ladder-iterative methods, such as forward-backward sweep, it is assumed that impedance of all lines and loads connected to each node is known, and source voltage, V_{source}, (which is typically a sub-station) remains known and fixed between iterations [9]. During forwards sweep, it is assumed that the circuit is under no-load condition, therefore, the voltage at the last

lateral is equal to V_{source}. Using this information, in a backward sweep, the load current is calculated at each node, using the below general equations [9].

$$I_{node} = \frac{V_{last\ node}}{Z} \tag{1.3}$$

$$V_{last\ node-1} = V_{last\ node} - I_{last\ node} \times Z_{last\ node} \tag{1.4}$$

In simple words, the radial system is solved two times, once with a fixed initial voltage profile and calculating currents injection in each node with given initial voltage, and second solving the voltage on each node with the previously calculated current injection. The analysis of a three-phase unbalanced system with a transformer requires detailed Y modelling with $3N \times 3N$ dimension [7]. Further, certain configurations of a three-phase transformer can lead to singularity issues in their admittance matrix [10]. In the text, these problems are addressed, and accurate modeling is developed on which HELM is applied.

1.4 Goal of the Thesis

In this thesis work, the following topics are discussed:

- Advantages and disadvantages of state-of-the-art PF methods.
- Basic modeling of system components, such as loads, buses, transformers for HELM application.
- Modeling of a three-phase radial distribution system.
- Application of Holomorphic embedding to balanced IEEE single-phase cases and its numerical simulation in MATLAB using MATPOWER [11-13].

- Application of Holomorphic embedding to unbalanced three-phase IEEE 37 feeder/bus system [14] and its numerical simulation in MATLAB. Discussing the limitation and HELM and future scope.

1.5 Organization of the Thesis

The chapter 2 elaborates on the literature review of iterative methods and ladder-iterative method for solving power flow. It also summarizes about Direct Approach method for solving power-flow in a three-phase distribution system. Further, the fundamentals of holomorphic embedding, analytic continuation and Pade` approximant is discussed in detail. The chapter 3 of the text elaborates on Holomorphic load embedding in a power system network. In the same chapter, a detailed numerical recursive model for a different type of buses and tap-changing transformer is formulated for single-phase and three-phase network. For easy understanding of the process of HELM, the chapter has a flow chart for the HELM procedure. The chapter 4 discusses simulation for various IEEE networks and a detailed step-by-step example for a three-bus system is discussed. The last chapter 5 discusses the conclusion of the work and future work for the HELM.

CHAPTER II

LITERATURE REVIEW & BACKGROUND

This Chapter will focus on the basic concept behind power flow, discuss traditional PF methods for single-phase equivalent network and for a radial distribution system. Further, it will discuss a non-iterative method of PF, such as Continuation Power Flow (CPF), DC approximation Power Flow and Holomorphic Embedded Load-flow (HELM) method. Further, the concept of Analytic Continuation and Pade` Approximants are discussed in detail.

2.1 Power Balance Equations

Out of four variable, voltage magnitude $|V_i|$, and voltage angle θ_I, net real power injection P_i, and net reactive power injection Q_i, at each bus in a power system network, two of them are directly or indirectly known during steady-state conditions. To study PF on any system, transmission line admittances and impedances, values of connected loads and their nature, and operating limit of transmission line, generator and other components is required. Using Kirchhoff Current Law, the nodal equation for the network as to be written as

$$I = Y \times V \tag{2.1}$$

where Y is a $N \times N$ admittance matrix, and I and V are current and voltage vector with $N \times 1$ dimensions. The nodal current equation for each bus i can be written as

$$I_i = \sum_{i=1}^{N} Y_{i,k} V_k \tag{2.2}$$

The net complex power delivered or Power balance equation at bus i can be written as

$$S_i = V_i I_i^* = P_i + jQ_i \tag{2.3}$$

Using the equation (2.2) and (2.3), the relation can be modified to

$$P_i + jQ_i = V_i \left[\sum_{k=1}^{N} Y_{i,k} V_k \right]^*, \forall i \tag{2.4}$$

Using the Euler form of the voltage terms [1], the equation (2.4) can be transformed into

$$P_i + jQ_i = V_i \sum_{k=1}^{N} Y_{i,k} V_k e^{(\delta_i - \delta\_k - \theta_{i,k})}, \forall i \tag{2.5}$$

The above PBE can be written in a trigonometric form as well as

$$P_i = V_i \sum_{k=1}^{N} Y_{i,k} V_k \, cos(\delta_i - \delta_k - \theta_{i,k}), \forall i \tag{2.6}$$

$$Q_i = V_i \sum_{k=1}^{N} Y_{i,k} V_k \, sin(\delta_i - \delta_k - \theta_{i,k}), \forall i \tag{2.7}$$

The equation (2.6) and (2.7) are used to iteratively calculate net complex power injection on each bus for given voltage magnitude and voltage angle, where $V_i = |V_i| \angle \theta_i$ and $V_i = |V_k| \angle \theta_k$.

2.2 Traditional Iterative Methods for Solving PF

One of the most common Iterative methods used in the industry is Newton-Raphson (NR) method, and the Fast Decoupled-NR method (FDNR). The methods such as Gauss-Seidel (GS) uses low memory and have slow convergence [2]. The process requires fixing the initial voltage guess, which is usually Voltage magnitude of 1.0 p.u. and voltage angle of 0 radians, termed as flat voltage profile. The PBE equation (2.4) can be written iteratively as shown below [15].

$$V_i(n+1) = \frac{1}{Y_{i,i}}\left[\frac{P_i - jQ_i}{V_i^*(n)} - \left(\sum_{k=1}^{N-1} Y_{i,k}\, V_k(n+1)\right) - \left(\sum_{k=i+1}^{N} Y_{i,k}\, V_k(n)\right)\right] \qquad 2.8$$

In the equation (2.8), $V_i(x)$ represents the value of the voltage at bus *i* for the xth iteration.

2.1.1 *Newton raphson method & others*

One of the most popular PF methods is the NR method. The first step is to initially set unknown variables, voltage magnitude and voltage angle on PQ bus and Reactive power injection and voltage angle for PV bus, with an initial guess. The values of the initial guess are generally flat voltage profile; however, the performance of the NR method depends on the topology of the network and how close is initial guess to the feasible solution in the solution plane. The second step includes writing a Taylor series form of PBEs with higher-order terms ignored, this step results in obtaining a linear system of equations for the system. The third step includes successive iterations of the obtained linearized PBEs which calculates the estimate of unknown variables. The decision of convergence is dependent on the iteration after which mismatch in values is smaller than set tolerance, generally 10^{-5}.

Mismatch equations are derived from the equation (2.6 and 2.7). The linearized system of equations for the n^{th} iteration is represented by the below equation (2.9)

$$\begin{bmatrix}\Delta\delta_i(n)\\ \Delta V_i(n)\end{bmatrix} = -J^{-1}\begin{bmatrix}\Delta P_i(n)\\ \Delta Q_i(n)\end{bmatrix} \quad 2.9$$

where $\Delta P_i(n)$ and $\Delta Q_i(n)$ is active and reactive power mismatch for n^{th} iteration for Bus i, the symbol J is Jacobian matrix [1]. The mismatch can be computed using the below equations (2.10) and (2.11).

$$\Delta P_i(n) = P_i(n) - |V_i(n)| \sum_{k=1}^{N} |V_k(n)| \left(G_{i,k}cos\theta_{i,k} + \mathrm{B_{i,k}}\sin\theta_{i,k}\right) \quad 2.10$$

$$\Delta Q(n) = Q_i(n) - |V_i(n)| \sum_{k=1}^{N} |V_k(n)| \left(G_{i,k}sin\theta_{i,k} - B_{i,k}cos\,\theta_{i,k}\right) \quad 2.11$$

The slack bus variables are removed from the matrix form of the linear system of equations as they are already known and assumed to be fixed as $V_{slack} = 1.0p.u.$ and $\theta_{slack} = 0$. The values of voltage magnitude and voltage angle for the $(n+1)^{th}$ iteration is calculated using the following equation:

$$\begin{bmatrix}\delta_i(n+1)\\ V_i(n+1)\end{bmatrix} = \begin{bmatrix}\delta_i(n)\\ V_i(n)\end{bmatrix} + \begin{bmatrix}\Delta\,\delta_i(n)\\ \Delta V_i(n)\end{bmatrix} \quad 2.12$$

The convergence rate for most topology is quadratic, however, the computational resources used in calculating Jacobian matrix and solving a linear system of equations for each iteration is substantial for larger power systems [2]. NR method works well for network operating near nominal load conditions but has poor performance for networks under heavily loaded conditions [16]. The reason to find a better PF method is due to two reasons, there is no guarantee of convergence after all the iterations as it depends on the starting point guess, and second that there are multiple operating solutions and there is no

control of its selection. NR method does not performance decreases in the distribution system due to radial nature of DS, higher Resistance (R) by Reactance (X) ratio, and introduction of mutual impedance between non-transposed phase conductor [7].

2.1.2 *Direct approach method for distribution system*

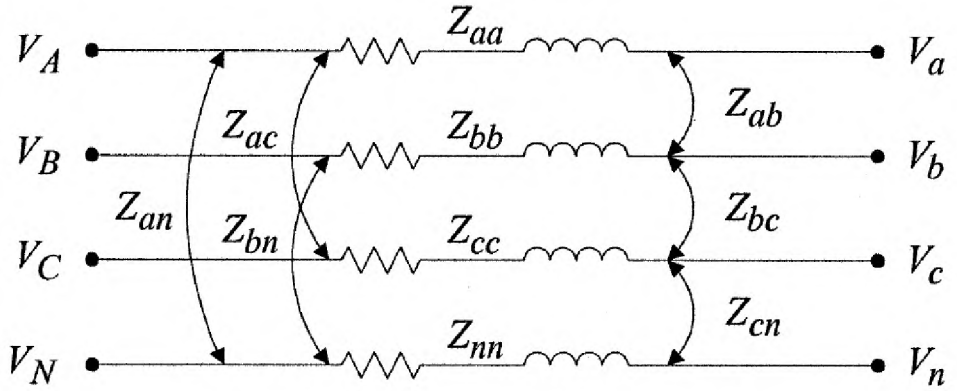

Figure 2 - Three-phase line model between two nodes.

Since, any distribution system is unbalanced due to non-ideal parameters like spacing between phase conductors, conductor sizing, and equal transposition among phases. The line impedances, for accurately modeling, uses modified Carson's equations of modeling line impedance [17]. The Carson's equations were published in 1926 which considered effects of self-impedance as well mutual impedance of nearby conductors in transmission line configuration. Figure 2 shows self-impedance and mutual impedance between phase conductors in a three-phase unbalanced transmission line. Using Kron reduction and Carson's equations, KVL for a simple two-node circuit can be represented by the below equations [18]:

$$\begin{bmatrix} V_A \\ V_B \\ V_C \end{bmatrix} = \begin{bmatrix} V_a \\ V_b \\ V_c \end{bmatrix} + \begin{bmatrix} Z_{aan} & Z_{abn} & Z_{acn} \\ Z_{ban} & Z_{bbn} & Z_{bcn} \\ Z_{can} & Z_{cbn} & Z_{ccn} \end{bmatrix} \begin{bmatrix} I_{Aa} \\ I_{Bb} \\ I_{Cc} \end{bmatrix} \quad 2.13$$

One method to find out load-flow in such radial distributed systems is called the Direct Approach algorithm [8]. The Direct approach method is based on which uses a bus-injection to branch-current (BIBC) and branch-current to bus-voltage (BCBV) matrices and bus-current injection to find out the load-flow parameters in the network. In the BIBC matrix, +1 in a row the bus-current injections contribute to the corresponding branch-current flow. In the below equation (2.14), the branch-current vector is represented by $[I_k^{Br}]$ with dimensions $(N-1)\times 1$, bus-current injection vector is I_i with dimensions $(N-1)\times 1$, where N is the number of nodes in the DS:

$$[I_k^{Br}] = [BIBC] \times [I_i] \tag{2.14}$$

It is important to note that in the I_i vector the source node or also known as substation node is not included as, in a radial distribution system, a source node is equivalent to a slack bus. Using the branch-current injections, it is straight to calculate node voltages in the radial DS using Ohm law. The equation (2.15)

$$[\Delta V] = [BCBV][I^{Br}] \tag{2.15}$$

where ΔV represents $V_1 - V_i$, with V_1 being the source node voltage. In the BCBV matrix, each row elements are filled with impedance values of the branch sections that current follow to reach a particular node. Using the equations (2.14) and (2.15), the below relation is derived:

$$[\Delta V] = [BCBV][BIBC][I] \tag{2.16}$$

The equation (2.16) can be iteratively represented as

$$[\Delta V^{n+1}] = [BCBV][BIBC][I^n] \tag{2.17}$$

$$[V^{n+1}] = \left[V^{intial}\right] + [\Delta V^{n+1}] \tag{2.18}$$

In a network, the BIBC matrix defines the relationship bus-current injection to branch-currents and BVBC defines the relationship between branch-current to bus voltages. These matrices are upper and lower triangles respectively and do not change for particular network topology, this feature makes this fast for approximate load-flow results in radial distribution systems [8].

2.2 Non-iterative method of PF

Iterative methods such as NR, Fast-decoupled NR, and others suffer through problems of convergence for heavily loaded systems and need a very good initial guess for finding a high voltage operable solution. They also suffer from higher computational requirements and becomes complexity exponentially increases as the power system size increases [20-21].

2.2.1 *Series power flow*

The series load-flow method tried to develop explicit power series of the bus voltage function. Two ways are discussed in the literature to achieve such closed-form, one by finding Taylor series coefficients via recursion technique and the other is fixed-point iteration [22]. This method uses real analysis as opposed to HELM which uses complex analysis, more detailed on which will be discussed in the next sections.

2.2.2 *Continuation power flow*

The Continuation Power Flow (CPF) method is based on the analysis technique of homotopy continuation which is characterized as path-following in nature. CPF is proven to work well for ill-conditioned and heavily loaded power systems and is also referred to as a predictor-corrector method. The voltage magnitude $|V_i|$ and voltage phase angle δ_i at

a bus i are unknown variable and a vector $z = (|V_i|, \delta_i)^T$. The PBE (2.10 and 2.11) can be expressed in term of variable z and the below homotopy equation would be:

$$H(z,t) = (1-t)(Z-a) + t\Delta P(n), \qquad \forall\, bus\ i \tag{2.19}$$

In the equation (2.19), for $t = 0$, $H(z,t) = Z - a$, where a is an intelligent initial guess for unknown variables and $t = 1$, the initial homotopy equation is recovered. CPF exploits the concepts of continuity and differentiation in a single domain, therefore is considered as a local method in terms of solution plane [4], [23].

2.2.3 *Holomorphic load flow method*

The most recently invented complex analysis method for calculating load method is load-flow is Holomorphic Load-Flow Method (HELM). It was invented by Dr. Antonio Trias and first presented in 2012 at the IEEE-PES conference [4]. It very well addresses the problem of iterative methods, faster convergence to a solution that is free from an initial guess, and lack of control over high-voltage solution selection in multi-solution situations. It guarantees a converged solution and unequivocally indicates, with oscillating Taylor series coefficients, if there is no solution for the set of non-linear set of power system equations.

HELM is a non-iterative method and turns voltage variables in PBEs into a complex analytic function, this enables a richer plane for solution finding, especially beyond the radius of convergence. The analytic function which is embedded with a holomorphic embedded parameter helps recursively calculate, at a well-known reference point called germ solution, the coefficients, $V_i[n]$, of Maclaurin power series. The analytic continuation is implemented using various near-diagonal Pade` approximant methods [24-25].

2.3 Analytical Continuation

Analytic continuation is a complex analysis technique that has properties to extend the domain of an analytic function beyond the original region of convergence (ROC) [4], [24]. Analytic continuation differs from numerical continuation as numerical continuation finds a solution which is interpolation to already know the solution in its nearby region. To apply HELM for a radial distribution system, an understanding of analytic continuation and Pade` approximants for power systems is necessary.

In context with HELM, the voltage in PBE equations is represented via an analytic function. To understand the concept of an analytic function, consider an example of power series $f(\alpha)$.

$$f(\alpha) = 1 + \alpha + \alpha^2 + \alpha^3 + \cdots \tag{2.20}$$

The series in equation (2.20) converges only for the values where $|\alpha| < 1$, which means that magnitude of the complex number α shall be less than 1 for the $f(\alpha)$ to be represented by the below expression:

$$g(\alpha) = \frac{1}{1-\alpha} \tag{2.21}$$

The function $g(\alpha)$ have a larger region of convergence than the original power series form of $f(\alpha)$, which is $real(\alpha) < 1$. The expression in equation (2.21) is commonly referred to as the closed-form of equation (2.20), which is easy to solve within the boundary of ROC but is not defined at $\alpha = 1$ or $\alpha \geq 1$.

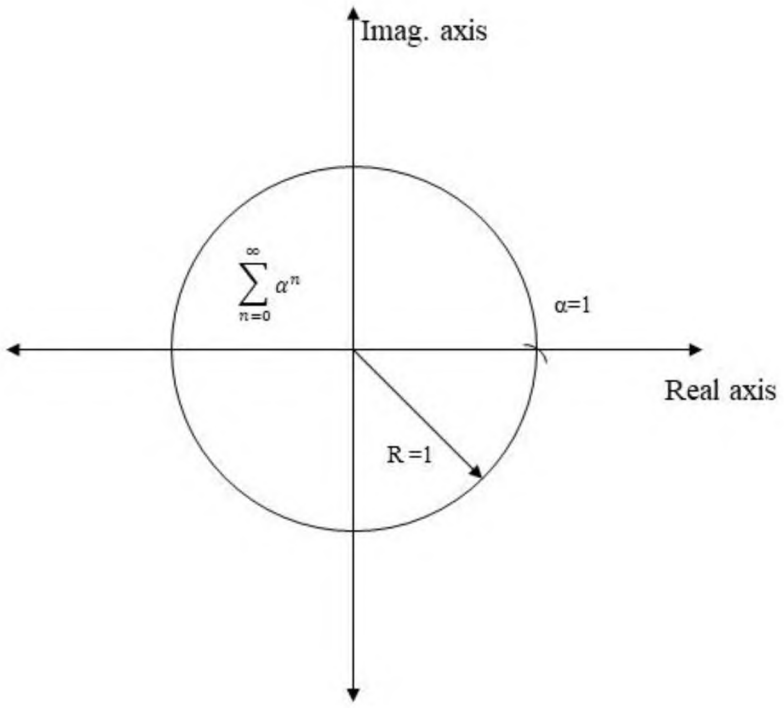

Figure 3 - Region of Convergence for a simple power series

Figure 3 gives a perspective of ROC for the equation (2.20). The equation (2.20) can further be expressed via an exponential function through analytic continuation by function $h(\alpha)$:

$$h(\alpha) = \int_0^{\infty} e^{-(1-\alpha)x} dx = lim \frac{e^{-(1-\alpha)x}}{-(1-\alpha)} \qquad 2.22$$

The region of convergence for function $h(\alpha)$ is everywhere, except $\alpha = 1$. There are various ways to extend the ROC of an algebraic function using analytics continuation. To find solutions for large sets of non-linear sets of equations, it is desirable to obtain maximum ROC, which can be obtained by employing maximal analytic continuation using Stahl's theory [19].

Using Taylor series expansion, more particularly Maclaurin series, a holomorphic or analytic function can be expressed by an infinite power series of the following form:

$$f(\alpha) = \sum_{n=0}^{\infty} c[n]\alpha^n = \frac{f^{(n)}(\alpha)}{n!}\alpha^n \qquad 2.23$$

where $c[n]$ is the nth coefficient term and $f^{(n)}(\alpha)$ is the nth derivative of function $f(\alpha)$at zero. The series from equation (2.23) has all the properties of an analytic function for infinite terms. However, in practical cases, dealing with infinite terms is computationally an NP-hard problem, therefore, a rational approximation method, such as Pade` approximant, needs to discuss in detail.

2.4 Pade` Approximant

The method to find the approximation of a function using rational function was developed by Henri Pade` in the year 1890. Pade` approximant is used to find out the approximate value of an infinite power series by finding its rational equivalent function. It is known that Pade` approximant can provide a better approximate value for function where the Taylor series does not converge or perform better for truncated Taylor series [25]. Therefore, Pade` approximants represent the holomorphic function and improve on ease to find the ROC of a power series [27]. The Pade` rational approximant with numerator L and denominator M as the degree is represented by

$$[L/M]f(\alpha) = \frac{\sum_{i=0}^{L} a[i]\alpha^i}{\sum_{j=0}^{M} b[j]\alpha^j} + o(\alpha^{L+M+1}) \qquad 2.24$$

Where $f(\alpha)$ is the analytic function, $o(\alpha^{L+M+1})$ represents the error caused due to truncation and $a[i]$ and $b[j]$ are the numerator and denominator coefficient for i^{th} and j^{th} coefficient. Pade` approximant is used to extrapolate the function domain beyond ROC for the Holomorphic/analytic function. When the ration of $L/M \cong 1$, which is

called diagonal or near-diagonal Pade` approximants, then the results obtained have the best accuracy [25]. There are various methods to solve Pade` approximants such as Viskovatov Method, Direct Matrix Method, and Epsilon Method (Wynn's Epsilon Method). For the scope of this text, the Direct Matrix Method is elaborated here.

2.4.1 Direct matrix method

Direct Matrix Method for calculating Pade` approximant where consider a Maclaurin power series in equation (2.25), which represents a holomorphic or analytic function, below:

$$c(\alpha) = c_0 + c_1\alpha^1 + c_2\alpha^2 + c_3\alpha^3 + \cdots$$

$$= \sum_{n=0}^{\infty} c[n]\alpha^n \qquad 2.25$$

where $c[n]$ represents the coefficient of the Maclaurin series and n represents the degree of the polynomial. The rational approximant for the series in the equation (2.25) is represented by equation (2.26) below.

$$[L/M]f(\alpha) = \frac{a_0 + a_1\alpha^1 + a_2\alpha^2 + a_3\alpha^3 + \cdots + a_L\alpha^L}{b_0 + b_1\alpha^1 + b_2\alpha^2 + b_3\alpha^3 + \cdots + b_M\alpha^M} \qquad 2.26$$

The equations (2.26) and (2.25) are equated as follows:

$$\frac{a_0 + a_1\alpha^1 + a_2\alpha^2 + a_3\alpha^3 + \cdots + a_L\alpha^L}{b_0 + b_1\alpha^1 + b_2\alpha^2 + b_3\alpha^3 + \cdots + b_M\alpha^M} = \sum_{n=0}^{\infty} c[n]\alpha^n \qquad 2.27$$

In the equation (2.27), $L + M + 1$ number of coefficients are known in the Maclaurin series of the holomorphic function and there are $L + M + 2$ number of unknown coefficients in Pade` approximant, this means that one coefficient in rational approximant

can be set as per the user, and in this text it, that variable is $b_0 = 1$. Further manipulating the equation (2.27), we get

$$a_0 + a_1\alpha^1 + a_2\alpha^2 + a_3\alpha^3 + \cdots + a_L\alpha^L =$$

$$(b_0 + b_1\alpha^1 + b_2\alpha^2 + b_3\alpha^3 + \cdots b_M\alpha^M)(c_0 + c_1\alpha^1 + c_2\alpha^2 + c_3\alpha^3 + \cdots \mathrm{c_{L+M}}\alpha^{\mathrm{L+M}}) \quad 2.28$$

The equation (2.28) can be represented by a system of M linear equations, as shown below:

$$\begin{gathered} b_M c_{L-M+1} + b_{M-1} c_{L-M+2} + \cdots b_0 c_{L+1} = 0 \\ b_M c_{L-M+2} + b_M c_{L-M+3} + \cdots b_0 c_{L+2} = 0 \\ \vdots \\ b_M c_L + b_{M-1} c_{L+1} + \cdots b_0 c_{L+M} = 0 \end{gathered} \qquad 2.29$$

At this point in the problem, the $c[n]$ are known and unknown is rational approximant's numerator and denominator variable a_n and b_n. The equation (2.28) can be represented in Matrix format as below:

$$\begin{bmatrix} c_{L-M+1} + c_{L-M+2} + \cdots C_L \\ c_{L-M+2} + c_{L-M+3} + \cdots c_{L+1} \\ \vdots \\ c_L + c_{L+1} + \cdots c_{L+M-1} \end{bmatrix} \begin{bmatrix} b_M \\ b_{M-1} \\ \vdots \\ b_1 \end{bmatrix} = \begin{bmatrix} c_{L+1} \\ c_{L+2} \\ \vdots \\ c_{L+M} \end{bmatrix} \qquad 2.30$$

Once the value of b_n are known, then through comparison of the power of α on both side of the equation (2.28), a_n can be calculated. The Direct Matrix method discussed in [24] can be used for any value of L and M, but through Stahl's theory, it is noted that diagonal or near-diagonal Pade` approximant results in maximum analytic continuation with largest ROC [19], [25]. Therefore, for the values of $L = M$ or $L \cong M$, the chances of getting maximal analytic continuation are higher.

2.5 Conclusion

Chapter II elaborates and prepares the basics of understanding HELM. The chapter dives into the basics of Power flow, details of traditional iterative and non-iterative methods for single-bus equivalent models as well for three-phase radial distribution systems. Further, the concept of ROC, analytic continuation and Pade` approximant were discussed. It was discussed a technique called Direct Matrix Method for solving Pade` approximant for a holomorphic function.

CHAPTER III

HOLOMORPHIC EMBEDDING LOAD-FLOW METHOD (HELM)

3.1 Introduction to HELM Modeling

By definition, a holomorphic function is a complex variable function that is differentiable at every complex point around a point in a complex plane. A general holomorphic function can be expressed by a convergent Taylor series at any point, and for the simplicity of the text, it is expressed at 0, thus a holomorphic function can be expressed as the Maclaurin series. Since expressing a holomorphic function with a closed-form expression is not accurate, therefore, the technique of holomorphic embedding is used in power balance equations and that makes sure that the resultant set of the equation is analytic or holomorphic. The process of embedding PBE is explained in detail in [25], [26].

3.2 HELM Model for Single-Phase Network

To develop the HELM model, consider a power system network of $N + 1$ buses, where there is 1 slack bus, set PQ of load buses, and set PV for generation buses. The PBE for the system can be summed with the following set of equations:

$$\sum_{k=0}^{N} Y_{i,k}V_k = \frac{S_i^*}{V_i^*}, i \in PQ \quad 3.1.1$$

$$P_i = Re\left(V_i \sum_{k=0}^{N} \left(Y_{i,k}V_k\right)^*\right), i \in PV \quad 3.1.2$$

$$|V_i| = V_{sp,i}, i \in PV \quad 3.1.3$$

$$V_{slack} = V_{sp,i}, i \in slack\ bus \quad 3.1.4$$

The equation (3.1.1) represents the PBE for a PQ bus, equations (3.1.2) and (3.1.3) represent the PV bus, and equation (3.1.4) represents the slack bus model. The equation (3.1.1) -(3.1.4) is not holomorphic and there is an infinite number of ways to transform them into one. Different holomorphic embedding results in a different set of the equation, but the solution shall be the same every time.

3.2.1 Basic holomorphic embedding

For holomorphically embedding and maintaining holomorphicity in the equation (3.1.1), it is restructured as below:

$$\sum_{k=0}^{N} Y_{i,k}^{trans} V_k(\alpha) = \frac{\alpha\, S_i^*}{V_i^*(\alpha^*)} - \alpha Y_i^{shunt} V_i(\alpha), i \in PQ \quad 3.2$$

The $Y_{i,k}$ matrix is divided into two parts, $Y_{i,k}^{trans}$ and Y_i^{shunt}, this helps in maintaining the holomorphicity of the function at $\alpha = 0, 1$. At $\alpha = 1$, the equation (3.2) is transformed back to the original PBE for a PQ bus. The equation (3.2.1) means that sum of all elements in a row of $Y_{i,k}^{trans}$ be 0, which is easy to solve. The Y_i^{shunt} includes shunt elements, such as tap-changing transformer, shunt admittance of transmission lines and

shunt capacitor or inductor at bus i. The term $V_k^*(\alpha)$ represents the holomorphic function for unknown voltage variables.

The slack bus voltage magnitude and voltage angle is a free variable and is generally set to a flat voltage profile for simplicity. Therefore, $V_{sp,i} = 1\angle 0°$, however for better systematic use of slack bus equation, the equation (3.1.4) is transformed into:

$$V_{slack} = 1 + \alpha\left(V_{sp,1} - 1\right) \tag{3.3}$$

The equation (3.1.2) can be embedded as follows:

$$\sum_{k=0}^{N} Y_{i,k}^{trans} V_k(\alpha) = \frac{\alpha P_i - jQ_i(\alpha)}{V_i^*(\alpha^*)} - \alpha Y_i^{shunt} V_i(\alpha), i \epsilon PV \tag{3.4.1}$$

$$V_i(\alpha) * V_i^*(\alpha^*) = 1 + \alpha\left(\left|V_{sp,i}\right|^2 - 1\right), i \in PV \tag{3.4.2}$$

The equation (3.4.1) represents the PBE equation for a generating bus and (3.4.2) represents the voltage condition for generating units.

3.2.2 Maclaurin power series for voltage function

The holomorphically embedded voltage function, $V_i(\alpha)$, is replaced by the Maclaurin power series to apply the analytic continuation technique to expand the ROC. The Maclaurin series can be expressed as below:

$$V(\alpha) = \sum_{n=0}^{inf} V[n]\,\alpha^n = V[0] + V[1]\alpha + V[2]\alpha^2 + \cdots V[n]\alpha^n \tag{3.5.1}$$

$$Q(\alpha) = \sum_{n=0}^{inf} Q[n]\,\alpha^n$$

$$= Q[0] + Q[1]\alpha + Q[2]\alpha^2 + \cdots Q[n]\alpha^n \tag{3.5.2}$$

where $V[n]$ are complex numbers and are recursively calculated. One important thing to note is that in equation (3.2), the $V^*(\alpha^*)$ is used, instead of $V^*(\alpha)$ or $V(\alpha^*)$. This is due to the requirement of voltage function needs to satisfy Cauchy-Reimann equations [4], [30]. The invalid holomorphic functions, $V^*(\alpha)$ and $V(\alpha^*)$, do not follow Weitinger's rule [28]. As per Weitinger's rule, the derivative of voltage function w.r.t. α^* $\left(\frac{\partial V}{\partial \alpha^*} = 0\right)$ shall be zero [28]. The $V^*(\alpha^*)$ is expressed in expanded form as below:

$$V^*(\alpha^*) = V^*[0] + V^*[1]\alpha + V^*[2]\alpha^2 + \cdots V^*[n]\alpha^n$$

Further, to compare the coefficients of power series in equation (3.2), (3.4.1) and (3.4.2), the embedded voltage function in the denominator needs to be taken care of by inversing the function $V(\alpha)$. Let, $W(\alpha)$ be the inverted function of $V(\alpha)$, which is defined as:

$$W(\alpha) = \frac{1}{V(\alpha)} = W[0] + W[1]\alpha + W[2]\alpha^2 + \cdots W[n]\alpha^n \qquad 3.6.1$$

$$W^*(\alpha^*) = \frac{1}{V^*(\alpha^*)} = W^*[0] + W^*[1]\alpha + W^*[2]\alpha^2 + \cdots W^*[n]\alpha^n \qquad 3.6.2$$

The equations (3.6) can be further manipulated by comparing coefficients like shown below:

$$\begin{gathered} W(\alpha) \times V(\alpha) = 1 \\ (W[0] + W[1]\alpha + \cdots W[n]\alpha^n) \times (V[0] + V[1]\alpha + \cdots V[n]\alpha^n) = 1 \\ W[0]V[0] = 1 \end{gathered} \qquad 3.7$$

The generalized form for inverted voltage function $W(\alpha)$, it defined in equation (3.8)

$$W[n] = -\frac{\sum_{l=1}^{n} V[l]W[n-l]}{V[0]} \qquad 3.8$$

The equation (3.8) is recursively used to calculate the value of $W[n]$ [33]. After substituting the values of power series in the equations (3.2), (3.3) and (3.4), they can be represented by:

$$\sum_{k=0}^{N} Y_{i,k}^{trans}\,(V_k[0] + V_k[1]\alpha + \cdots V_k[n]\alpha^n)$$

$$= \alpha S_i^*(W_i[0] + W_i[1]\alpha + \cdots W_i[n]\alpha^n)$$

$$- \alpha Y_i^{shunt}(V_i[0] + V_i[1]\alpha + \cdots V_i[n]\alpha^n), i \in PQ \qquad 3.9.1$$

$$\sum_{k=0}^{N} Y_{i,k}^{trans}\,(V_k[0] + V_k[1]\alpha + \cdots V_k[n]\alpha^n)$$

$$= \big(\alpha P_i - j(Q_i[0] + Q_i[1]\alpha + \cdots Q_i[n]\alpha^n)\big)\big((W_i[0] + W_i[1]\alpha + \cdots W_i[n]\alpha^n)\big)$$

$$- \alpha Y_i^{shunt}(V_i[0] + V_i[1]\alpha + \cdots V_i[n]\alpha^n), i \in PV \qquad 3.9.2$$

$$(V_i[0] + V_i[1]\alpha + \cdots V_i[n]\alpha^n)(V_i^*[0] + V_i^*[1]\alpha + \cdots V_i^*[n]\alpha^n) = 1 + \alpha\left(\left|V_{sp,i}\right|^2 - 1\right), i$$

$$\in PV \qquad 3.9.3$$

Once, the coefficients in the above equations are equated on LHS and RHS, the equations (3.9) can further be represented by:

$$\sum_{k=0}^{N} Y_{i,k}^{trans}\,V_k[n] = S_i^* W_i^*[n-1] - Y_i^{shunt} V_i[n-1], i \in PQ \qquad 3.10$$

$$\sum_{k=0}^{N} Y_{i,k}^{trans}\,V_k[n]$$

$$= P_i W_i^*[n-1] - j\left(\sum_{l=0}^{n} Q_i[l] W_i^*[n-l]\right) - Y_i^{shunt}[n-1], i\epsilon PV \qquad 3.11$$

$$V_i^{real}[0] = 1$$

$$V_i^{real}[1] = \frac{V_i^{sp^2} - 1}{2}$$

$$2V_i^{real}[n] = -\sum_{l}^{n-1} V_k[l]V_k^*[n-l], n \geq 2, l \geq 1, i \in PV \quad 3.12$$

3.2.3 Germ solution

At $\alpha = 0$, the equations for PQ bus, PV bus and the slack bus turn into the following:

$$\sum_{k=0}^{N} Y_{i,k}^{trans} V_k[0] = 0, i \in PQ \quad 3.13.1$$

$$V_{slack} = 1\angle 0° \quad 3.13.2$$

$$\sum_{k=0}^{N} Y_{i,k}^{trans} V_k[0] = -jQ_i[0]W_i^*[0], i \in PV \quad 3.13.3$$

$$V_i[0]V_i^*[0] = 1, i \in PV \quad 3.13.4$$

Solving the germ equations using any method for solving a set of linear equations would obtain the germ solution, at each bus of the system it is going to be $V_i[0] = 1\angle 0°$, $W_i[0] = 1$ and $Q_j[0] = 0, j \in PV$ [24]. For any value of α, other than 0, the function of voltage needs to be expressed in Maclaurin power series, where recursively obtain the coefficient of the Maclaurin power series and then develop analytic continuation using Pade` approximant for the said series. The iterative methods are generally defined as methods that successively or iteratively displaces from the center while finding the solution. The HELM does not fall into the iterative method definition, therefore, the best way to describe HELM is using the term recursively. Therefore, HELM recursively solves the consistent system of equations (3.10), (3.11), and (3.12) along with germ solution gives the complex values of power series coefficients.

The holomorphic equations and the unknown voltage power series coefficients are complex-valued numbers and need to be separated into real and imaginary parts for recursively solving through a linear system of equations as PV and PQ bus equations are coupled together [25].

3.2.4 Tap-changing and phase-shifting transformer

In the complex IEEE standard power system model cases like the 118-Bus case, the phase-shifting transformers with tap-ratio τ parameter are introduced. Since the τ parameter introduces an asymmetry in the Y^{trans}. To get the same flat voltage profile as mentioned in germ equation (3.13.1), the Y^{trans} needs to be separated into Y_{sym}^{trans} and a diagonal matrix Y^{shunt} [29]. In Figure 3, the total line charging susceptance $jBc/2\ \Omega$ is expressed in the π-network model configuration. Without the tap-changing or phase-shifting transformer, an admittance matrix, in its canonical form, is:

$$Y = \begin{bmatrix} (Y_s + j0.5 * Bc)/\tau^2 + Y_{sh} & -Y_s/\tau^* \\ -Y_s/ & Y_s \end{bmatrix} \qquad 3.14$$

The equation (3.14) is a complete admittance matrix containing series admittance, Y_s, shunt susceptance, Bc, and shunt admittance, Y_{sh}. Figure-3 shows the elements of a tap-changing transformer between two buses.

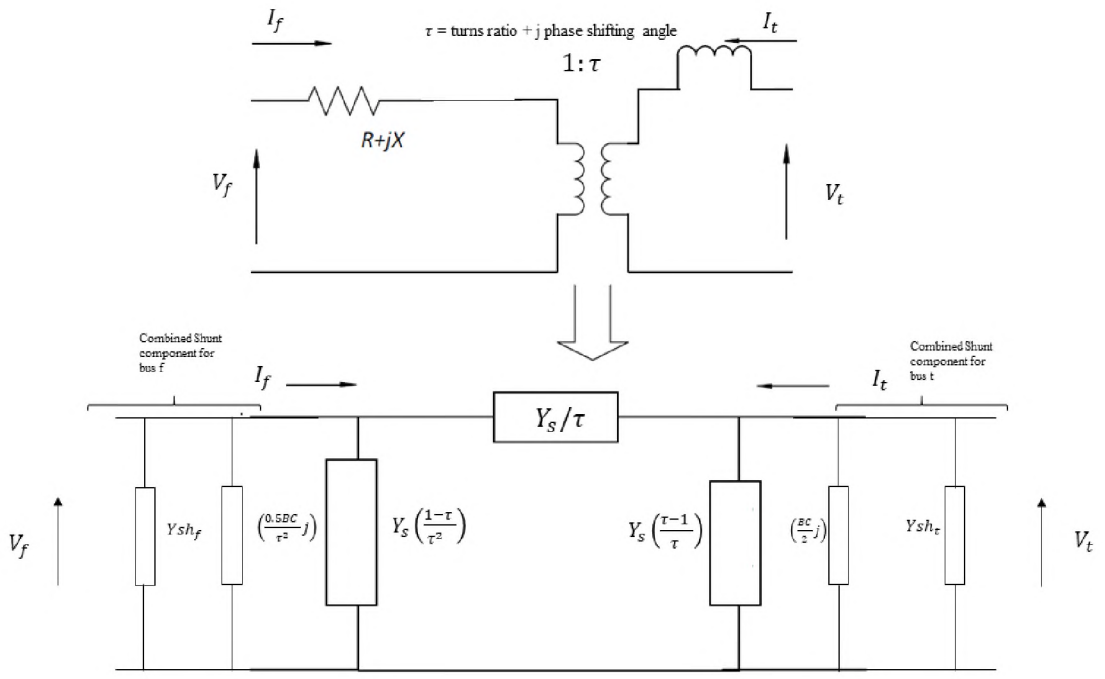

Figure 4- Equivalent Model of a bus with a Tap & Shift-changing transformer

The matrix below Y_{sym}^{trans} complies with the equation (3.13.1) and therefore can be used to calculate germ solution easily. The equation (3.15.2) represents the final shunt component on admittance at a bus, it contains connected shunt reactance and capacitance at a bus, line susceptance $j\,Bc$, and tap-changing transformer effect [31].

$$Y_{sym}^{trans} = \begin{bmatrix} Y_s/\tau^* & -Y_s/\tau^* \\ -Y_s/ & Y_s \end{bmatrix} \qquad 3.15.1$$

$$Y^{shunt} = \begin{bmatrix} Y_{sh} + j\left(\frac{Bc}{2}\right) + \left(Y_s\left(\frac{1-\tau}{\tau^2}\right)\right) & 0 \\ 0 & Y_{sh} + j\left(\frac{Bc}{2}\right) + \left(Y_s\left(\frac{\tau-1}{\tau}\right)\right) \end{bmatrix} \qquad 3.15.2$$

It is important to note that τ, is a complex number, where the magnitude of the τ

represents the tap-ratio and the polar angle of the τ represents the phase shift angle of the transformer. The below set of the equation represents the Holomorphic embedded PBE and are based on equation (3.15).

$$\sum_{k=0}^{N} Y_{sym,i,k}^{trans} V_k[n] = S_i^* W_i^*[n-1] - Y_i^{shunt} V_i[n-1], i \in PQ \qquad 3.16.1$$

$$\sum_{k=0}^{N} Y_{sym,i,k}^{trans} V_k[n]$$

$$= P_i W_i^*[n-1] - j\left(\sum_{l=0}^{n} Q_i[l] W_i^*[n-l]\right)$$

$$- Y_i^{shunt}[n-1], i \epsilon PV \qquad 3.16.2$$

$$V_i^{real}[0] = 1\ ,\ V_i^{real}[1] = \frac{V_i^{sp^2}-1}{2}$$

$$2V_i^{real}[n] = -\sum_{l}^{n-1} V_k[l] V_k^*[n-l], n \geq 2\ , l \geq 1, i \in PV \qquad 3.16.3$$

At $\alpha = 0$, the system of equation in (3.16) can be calculated using:

$$\sum_{k=0}^{N} Y_{sym,i,k}^{trans} V_k[0] = 0, i \in PQ \qquad 3.17.1$$

$$V_{slack}[0] = 1\angle 0° \qquad 3.17.2$$

$$\sum_{k=0}^{N} Y_{sym,i,k}^{trans} V_k[0] = -jQ_i[0] W_i^*[0], i \in PV \qquad 3.17.3$$

$$V_i[0] V_i^*[0] = 1, i \in PV \qquad 3.17.4$$

Further, the embedded equations are split into real and imaginary parts. The voltage variable, $V_i[n]$, is split into $V_i^{re}[n]$ and $V_i^{im}[n]$. Similarly, elements of the admittance

matrix, $Y_{i,k}$, is split into $(G_{i,k} + jB_{i,k})$, and complex power S_i is split into P_i and Q_i. This increases the dimensions of each matrix in holomorphically embedded PBE by two times. This step is necessary as the real part and imaginary part of the unknown voltage variable is both unknown and needs to be solved by solving a set of linear equations [25].

3.3 HELM Model for Three-Phase Network

For the development of the HELM model for the three-phase radial distribution network, voltage regulator and substation transformer has been removed, where substation transformer is assumed to be Slack bus. Each bus in a three-phase network can have either one phase, two-phase or three-phase laterals/nodes. As discussed in Section 2.1, an admittance matrix for a three-phase distribution system is made up of a Phase-frame matrix rather than a symmetrical element [7], [32].

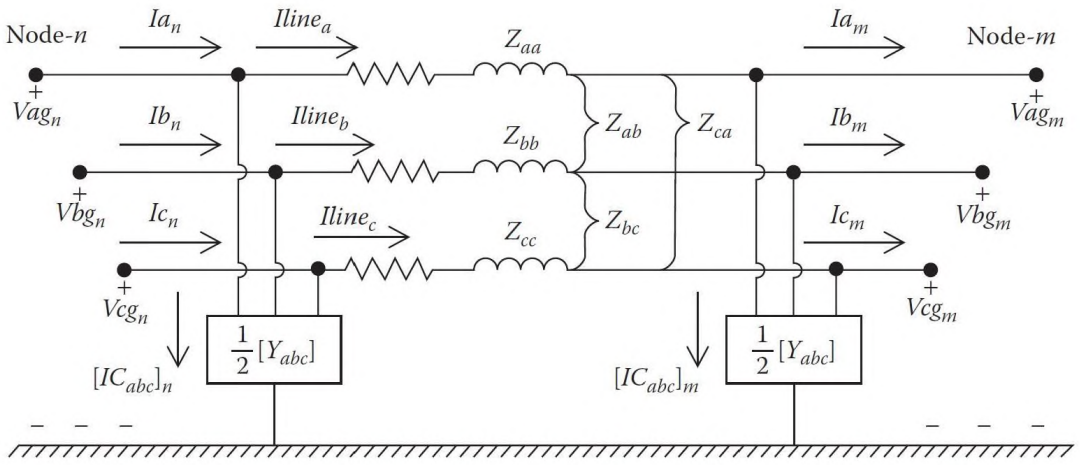

Figure 5 – Three-phase line model with series and shunt components

There are various kinds of electrical loads in a power system. The kinds are a primarily non-linear combination of constant impedance (Z), constant power(P) and

constant current (I) loads, more commonly referred to as ZIP loads. Below Table (2) summarizes the relation between ZIP and bus voltage in Delta and Wye connected loads:

Table 2 – Modeling for ZIP loads in PBEs

Load Type	Current Injection as a function of Bus Voltage	Wye Load
Constant Impedance	$I_{i,Z}^{abcn}(V_i)$	$-\left(\frac{S_{i,Nominal}^{abcn}}{V_i^{abcn}}\right)^*$
Constant Current	$I_{i,I}^{abcn}(V_i)$	$\frac{-V_i^{abcn}}{\lvert V_i^{abcn}\rvert} I_{i,Nominal}^{abcn}$
Constant Power	$I_{i,PQ}^{abcn}(V_i)$	$-Y_{i,Nominal}^{abcn} V_i^{abcn}$

In Table (2), terms with nominal in subscript represent the values for 1.0 per unit voltage [34]. It is relevant to note that constant impedance load has an inverse relation with bus voltage, which means that any drop in voltage would increase net current injection. Similarly, for constant power loads, the bus voltage has a direct relation to bus current. Figure (5) is accurate modeling of three-phase transmission lines with buses n and m. The process of calculating parameter for three-phase lines can be summarized as below [7], [10]:

$$\begin{bmatrix} V_n^{abcn} \\ I_n^{abcn} \end{bmatrix} = \begin{bmatrix} [I] + \frac{1}{2}[Z^{abc}][Y^{abc}] & Z^{abc} \\ [Y_{abc}] + \frac{1}{4}[Y^{abc}][Z^{abc}][Y^{abc}] & [I] + \frac{1}{2}[Y^{abc}][Z^{abc}] \end{bmatrix} \begin{bmatrix} V_m^{abcn} \\ I_m^{abcn} \end{bmatrix} \qquad 3.18$$

The equation (3.18) is analogous to the ABCD parameter model in transmission line analysis. It is to note that in equation (3.18) each ABCD parameter is itself a 3×3 matrix instead of a single element. The relation in equation (3.18) is useful in algorithms that work on the ladder technique for solving the power-flow problem, as the voltage on the

next bus can be determined by using the voltage at the previous bus in a radial network [32]. Also, the line-to-line quantities can be, vice versa, calculated using the phase-to-neutral quantities using the below relations:

$$\begin{bmatrix} V_{ab} \\ V_{bc} \\ V_{ca} \end{bmatrix} = \begin{bmatrix} 1 & -1 & 0 \\ 0 & 1 & -1 \\ -1 & 0 & 1 \end{bmatrix} \begin{bmatrix} V_{an} \\ V_{bn} \\ V_{cn} \end{bmatrix} \quad 3.19.1$$

$$\begin{bmatrix} I_{an} \\ I_{bn} \\ I_{cn} \end{bmatrix} = \begin{bmatrix} 1 & 0 & -1 \\ -1 & 1 & 0 \\ 0 & -1 & 1 \end{bmatrix} \begin{bmatrix} I_{ab} \\ I_{bc} \\ I_{ca} \end{bmatrix} \quad 3.19.2$$

The above equation (3.19) is derived from Kirchhoff's voltage and current laws.

3.3.1 HELM for wye-connected PQ loads

For a three-phase radial distribution system, each bus can have up to three nodes corresponding to the a, b, and c phase, for the programming point of all the nodal quantities in each bus are transformed into a system-wide vector. Such a vector quantity would have $(3n) \times 1$ dimension. Similarly, a system-wide admittance matrix can be formed with each row and each column corresponding to the phase node of a bus with dimensions of $(3n) \times (3n)$, where n is the number of buses in the three-phase system. Since in the modified case, a three-phase transformer is opted out, Y^{shunt} is zero. For example, the two-bus system in equation (3.20.1) has three-phase nodes each, each node is addressed with 1-6 number.

$$\begin{array}{lccc} Bus\ Id \leftrightarrow Phase\ A & Phase\ B & Phase\ C \\ Bus\ 1 \rightarrow & 1 & 2 & 3 \\ Bus\ 2 \rightarrow & 4 & 5 & 6 \end{array} \quad 3.20.1$$

The total six-phase nodes are arranged in a linear manner for vector calculations, as shown in the equation (3.20.2):

$$\begin{matrix} Bus\ Idx & Linear\ Phase\ node\ idx \\ Bus\ 1 & \begin{cases} 1 \\ 2 \\ 3 \end{cases} \\ Bus\ 2 & \begin{cases} 4 \\ 5 \\ 6 \end{cases} \end{matrix} \quad 3.20.2$$

The equation (3.21.1) below represents PBEs for constant power loads connected in the Wye connection. After holomorphically embedding, the recursive relation for calculating the power series coefficient is obtained in the equation (3.21.1).

$$\sum_{k=0}^{3N} Y_{i,k}\, V_k(\alpha) = \alpha \frac{S_i^*}{V_i^*(\alpha^*)}, i \in PQ\ nodes \quad 3.21.1$$

$$\sum_{k=0}^{3N} Y_{i,k}(V_k[0] + V_k[1]\alpha^1 + V_k[2]\alpha^2 + \cdots + V_k[n]\alpha^n) = \alpha S_i^*(W_i^*[0] + W_i^*[1]\alpha^1 + W_i^*[2]\alpha^2 \ldots + W_i^*[n]\alpha^n),\ i \in PQ \quad 3.21.2$$

$$\sum_{k=0}^{3N} Y_{i,k} V_k[n] = S_i^* W_i^*[n-1] \quad 3.21.3$$

The germ solution for a 1 bus with three-phase nodes which are Wye connected PQ loads can be expressed as below:

$$\sum_{k=0}^{3N} Y_{sym,i,k}^{trans}\ V_i^{abcn}[0] = V_i^{abcn,0} \quad 3.17.1$$

The vector $V_i^{abcn,0}$ represent nominal or balanced three-phase voltage, admittance matrix is made of phase-frame nodal admittance sub-matrices.

3.3.2 *HELM for wye-connected constant impedance loads*

The impedance loads, such as heating load, can be modeled using the below expression:

$$\sum_{k=0}^{3N} Y_{i,k}\, V_k(\alpha) = \alpha \frac{V_i^*(\alpha^*)}{Z_i}, i \in \text{set of constant impedance nodes} \qquad 3.18$$

where $Z_i = \frac{|V_i^{nom}|^2}{S_i^*}$ and V_i^{Nom} stands for the nominal phase-to-neutral voltage for node i and it is a constant value for a system. The nominal voltage depends upon phase a, b, or c of the node. The equation (3.18) can be modified to a recursive relation for calculating voltage series coefficient:

$$\sum_{k=0}^{N} Y_{i,k}\, V_k[n] = \frac{S_i^* V_i^*[n-1]}{|V_i^{nom}|^2}, i \in \text{set of constant impedance nodes} \qquad 3.19$$

3.3.3 *HELM for wye-connected constant current loads*

For constant current loads, the PBE equation for wye-connected three-phase loads can be embedded as below:

$$\sum_{k=0}^{N} Y_{i,k}\, V_k(\alpha) = \alpha I_i(\alpha) \qquad 3.20.1$$

$$\sum_{k=0}^{N} Y_{i,k}(V_k[0] + V_k[1]\alpha^1 + V_k[2]\alpha^2 \ldots + V_k[n]\alpha^n)$$

$$= (I_i[0]\alpha^1 + I_i[1]\alpha^2 + I_i[2]\alpha^3 \ldots + I_i[n]\alpha^{n+1}) \qquad 3.20.2$$

In the equation (3.20.2), power on both sides is compared and a recursive relationship is defined below:

$$\sum_{k=0}^{N} Y_{i,k} V_k[n] = I_i[n-1] \qquad 3.20.3$$

Therefore, using the equations the set of holomorphically embedded equations for wye connected three-phase load an accurate power flow can be calculated for various combinations of loads.

3.4 Flow Chart of the HELM

Figure (6) describes the steps for the HELM algorithm for single-phase and three-phase power systems. It starts with reading the data such as

For single-bus cases:

- Bus Data includes bus id, bus type, complex power demand on the bus, connect shunt equipment.
- Generation Data includes bus id with generating units, complex power generation capacity, set voltage at buses, maximum and minimum complex power limit.
- Branch Data includes "From" and "To" bus pairing, series and shunt impedance off the branches, and tap-changing ratio.

For three-phase radial unbalanced network:

- Branch/line Data includes "From" and "To" nodes for each phase, length of the conductor, and transmission line pole configuration.
- Spot Load Data includes the type of load, complex power load for each node.
- Network Elements Data includes data for the voltage regulator and three-phase transformer.

After reading the data, it is manipulated in the form for programming use. The bus admittance matrix Y is calculated for the network configuration. The admittance matrix remains constant for a network case. For a single-phase equivalent case, the size of Y is $n \times n$, and for a three-phase network, the size is $3n \times 3n$, where n is the

number of buses in the system. The right side of holomorphic embedded PBE is set to zero for calculating Germ solution, which is coefficient $V[0]$ of the voltage power series. In the next step, $V[n]$ the coefficient for each bus is calculated using $V[n-1]$ coefficient. This recursive relationship is based on equations (3.10-3.12). Once the power series coefficients are obtained for a predefined value of n, like 50. Then, the Maclaurin series representation of voltage at each bus is expressed as a rational approximation using Pade` approximant technique. After this step, the mismatch is checked for each bus between the given net power injection and net power injection calculated using the obtained voltage value using the following relation:

$$mismatch = \left| S_i - \left(V_i \left(\sum_{k=0}^{N} Y_{i,k} V_k \right)^* \right) \right| \qquad 3.21$$

Mismatch value is further divided into real power mismatch and reactive power mismatch for different bus types.

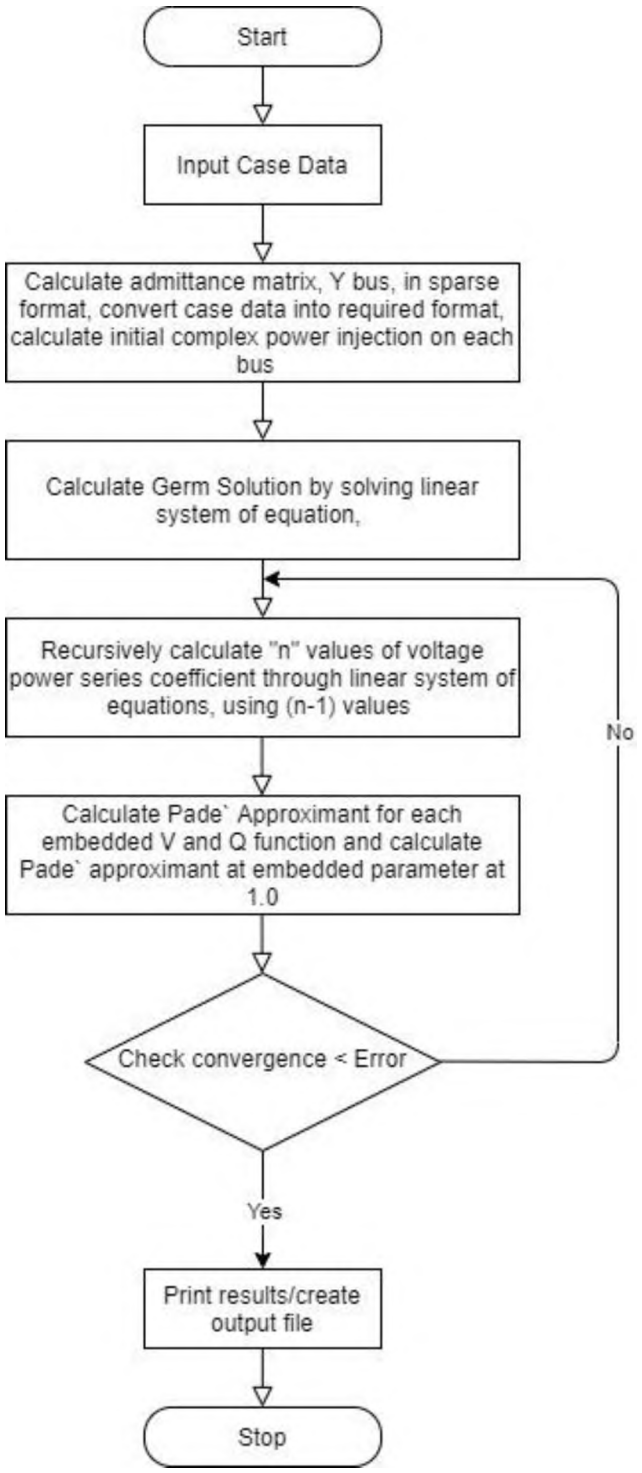

Figure 6 – Steps for Implementing HELM

3.5 Summary

The iterative methods (also known as Numerical methods) of load-ow analysis have convergence problems due to the fractal shape of the basin of attraction of the solution map. Due to a lack of knowledge regarding general characteristics of shape and size of the said basins, the Holomorphic Embedding Load-Flow method calculates the coefficients of the voltage series with an embedding reference point as the germ solution. The voltage power series is one of the major ways of representing the Holomorphic functions. The obtained Power series only converge within the radius of convergence (ROC), however, using an analytic continuation, such as near-diagonal sequences of Pade approximants, the region of convergence is extended beyond the ROC.

CHAPTER IV

SIMULATIONS

4.1 Convergence Criteria

In the entire project, a per-unit system is used for all the power system values. The complex power base selected was 100 MVA. The MATPOWER package [11-13] and Julia v1.1.1 [35] are employed to conduct the simulations. The stopping criteria for the Pade` approximant values for the bus voltage magnitude are set to 10^{-4} per unit and for voltage angle is set to 0.5 degrees. Further, the tolerance for stopping criteria for power mismatch on all buses is set to 10^{-6} per unit. The algorithms have been implemented in IEEE standard bus cases [36].

4.2 Simulation Results

This section explains and summarizes the load-flow results using the holomorphic load-flow method. The bus cases selected are diverse with a variety of loads, generation capacity, branch parameter, tap-changing, and phase-shifting transformers. All the solutions solved using HELM have been verified with the traditional Newton-Raphson method. This work only records the variation of number terms in power series required for reducing power mismatch. For future work, variation in the L/M ratio of Pade` approximant can also be examined for various IEEE standard cases.

4.2.1 Single-phase bus systems

The single-phase cases are the equivalent representation of a three-phase balanced power system network. The solution is extrapolated to the other two phases after calculating the solution for the single-phase equivalent. This assumption is particularly useful for DC approximated power-flow methods and a very large power grid model.

4.2.1.1 IEEE 5-bus system

A modified IEEE 5-bus case which has a tap-changing and phase-shifting transformer on the branch 3-4. The data for the case is shared in Annexure A. The below equation (4.1-4.3) represents the calculated bus admittance matrix Y. The matrix Y is split into the series matrix Y^{trans} and shunt matrix Y^{shunt}.

$$Y = \begin{bmatrix} 22.250 - j222.484 & -3.523 + j\,35.234 & 0.0 + j0.0 & -3.2569 + j32.569 & -15.4703 + j154.703 \\ -3.523 + j35.234 & 12.691 - j126.898 & -9.1676 + j\,91.676 & 0.0 + j0.0 & 0.0 + j\,0.0 \\ 0.0 + j0.0 & -9.1676 + j91.676 & 9.1676 - j95.489 & -0.517 + j2.936 & 0.0 + j0.0 \\ -3.257 + j32.569 & 0.0 + j0.0 & 0.5177 + j2.936 & 6.590 - j68.224 & -3.333 + j33.336 \\ -15.470 + j154.70 & 0.0 + j0.0 & 0.0 + j\,0.0 & -3.3336 + j33.336 & 18.804 - j188.021 \end{bmatrix} \quad 4.1$$

$$Y^{trans} = \begin{bmatrix} 22.2507 - j222.507 & -3.52348 + j35.235 & 0.0 + j0.0 & -3.2569 + j32.569 & -15.470 + j154.703 \\ -3.52348 + j35.235 & 12.6911 - j126.911 & -9.16758 + j91.676 & 0.0 + j0.0 & 0.0 + j0.0 \\ 0.0 + j0.0 & -9.1676 + j91.676 & 9.68532 - j94.612 & -0.5178 + j2.9362 & 0.0 + j0.0 \\ -3.257 + j32.569 & 0.0 + j0.0 & 0.51774 + j2.9362 & 6.07284 - j68.8419 & -3.33367 + j33.337 \\ -15.4703 + j154.703 & 0.0 + j0.0 & 0.0 + j0.0 & -3.3337 + j33.337 & 18.804 - j188.04 \end{bmatrix} \quad 4.2$$

$$Y^{Shunt} = \begin{bmatrix} 0.0 + j0.02248 \\ 0.0 + j0.01282 \\ -0.51773 - j0.876976 \\ 0.517735 + j0.617297 \\ 0.0 + j0.019 \end{bmatrix} \quad 4.3$$

The set of equations (3.16) can be separated in real and imaginary component for calculation and can be written as below for IEEE 5-bus system.

$$\begin{bmatrix} 222.51 & 0.0 & -35.2348 & -3.5235 & 0.0 & 0.0 & -32.569 & -3.2569 & -154.703 & 0.0 \\ 22.251 & 1.0 & -3.5235 & 35.2348 & 0.0 & 0.0 & -3.2569 & 32.569 & -15.4703 & 0.0 \\ -35.235 & 0.0 & 126.911 & 12.691 & -91.6758 & 0.0 & 0.0 & -0.0 & 0.0 & 0.0 \\ -3.525 & 0.0 & 12.6911 & -126.911 & -9.16758 & 0.0 & 0.0 & 0.0 & 0.0 & 0.0 \\ 0.0 & 0.0 & -91.675 & -9.168 & 94.6121 & 0.0 & -2.936 & -0.5177 & 0.0 & 0.0 \\ 0.0 & 0.0 & -9.1675 & 91.6758 & 9.68532 & 1.0 & -0.5178 & 2.93622 & 0.0 & 0.0 \\ 0.0 & 0.0 & 0.0 & 0.0 & 0.0 & 0.0 & 0.0 & 1.0 & 0.0 & 0.0 \\ 0.0 & 0.0 & 0.0 & 0.0 & 0.0 & 0.0 & 1.0 & 0.0 & 0.0 & 0.0 \\ -154.703 & 0.0 & 0.0 & 0.0 & 0.0 & 0.0 & -33.33 & -3.334 & 188.04 & 0.0 \\ -15.4703 & 0.0 & 0.0 & 0.0 & 0.0 & 0.0 & -3.333 & 33.334 & 18.804 & 1.0 \end{bmatrix} \begin{bmatrix} V_1^{im}[n] \\ Q_1[n] \\ V_2^{im}[n] \\ V_2^{re}[n] \\ V_3^{im}[n] \\ Q_3[n] \\ V_4^{im}[n] \\ V_4^{re}[n] \\ V_5^{im}[n] \\ Q_5[n] \end{bmatrix}$$

$$= \begin{bmatrix} Im.(RHSof3.16.2) \\ Re.(RHSof3.16.2) \\ Im.(RHSof3.16.1) \\ Re.(RHSof3.16.1) \\ Im.(RHSof3.16.2) \\ Re.(RHSof3.16.2) \\ 0.0 \\ 1.0 \\ Im.(RHSof3.16.2) \\ Re.(RHSof3.16.2) \end{bmatrix}$$

$$- \begin{bmatrix} 22.251 & 0.0 & -15.4703 \\ -222.507 & 0.0 & 154.703 \\ -3.52348 & -9.16758 & 0.0 \\ 35.2348 & 91.6758 & 0.0 \\ 0.0 & 9.68532 & 0.0 \\ 0.0 & -94.6121 & 0.0 \\ 0.0 & 0.0 & 0.0 \\ 0.0 & 0.0 & 0.0 \\ -15.4703 & 0.0 & 18.804 \\ 154.703 & 0.0 & -188.04 \end{bmatrix} [V_1^{re}[n] \quad V_3^{re}[n] \quad V_5^{re}[n]] \qquad 4.4$$

Using the steps explained in section 3.4, the equation (4.4) is solved recursively solved to obtain coefficients of the power series. The coefficients are further used to find the solution using Pade` approximant. Table (3) shows the power flow results for the IEEE 5-bus system using HELM.

Table 3 – Power-Flow Solution for Modified IEEE 5-Bus Case

Bus Id	Bus Type	Voltage Magnitude	Voltage Angle	Net MW Injection	Net MVar Injection
1	PV	1	3.485	210	29.404
2	PQ	0.989371	-0.182	-300	-98.61
3	PV	1	0.223	23.49	178.737
4	REF	1	0	-395.01	-1.863
5	PV	1	4.286	466.51	-37.606

Further power-flow results are mentioned below:

Total Mw Generated = 1004.99 Total MVar Generated = 398.753

Total Mw Load = 1000.0 Total MVar Load = 328.69

Total Mw Loss = 4.99 Total MVar Loss = 70.063

Mw Shunt Losses: -0.0 MVar Shunt Losses:0.0

	Maximum:	Minimum:
Voltage Mag:	1.0	0.989370564606465
Voltage Ang:	4.286438009999222	-0.1828905259805847

Coefficients in Voltage series = 40 Number of Buses = 5

Convergence Status = true Number of Branches = 6

Initial condition = Flat Start Mismatch Value = 4.39648317751562e-14

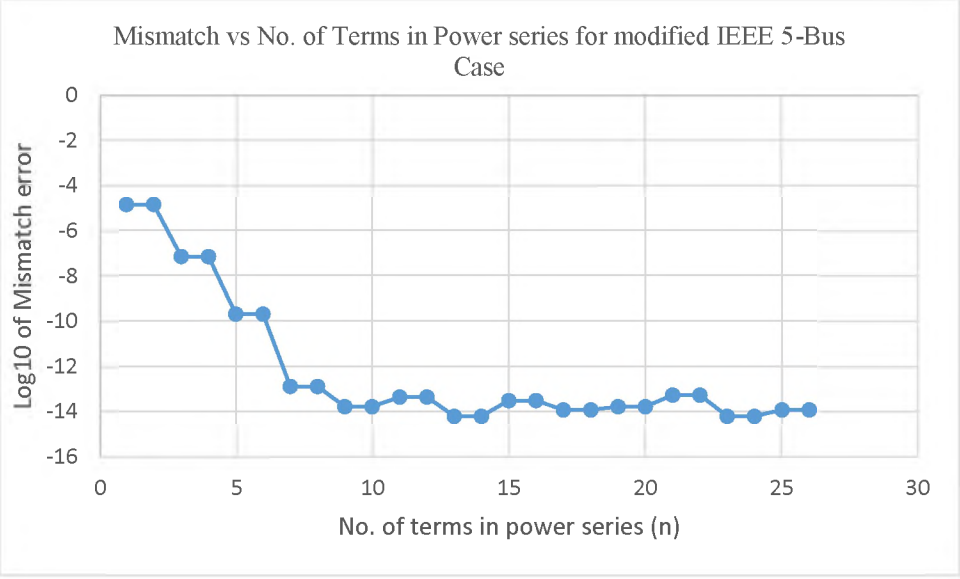

Figure 7 – Highest Absolute Mismatch of PBE vs Number of terms in Power series for Modified IEEE 5-Bus Case

Figure (7) shows the decreasing trend of mismatch error with an increase in power series terms. It can be noted that mismatch error is almost constant for power series coefficient, $n > 10$. Therefore, for better computational performance for IEEE 5-bus system power series terms shall be set of 10.

4.2.1.2 IEEE 33bw-bus system

The IEEE 33bw-bus system is shown in Figure (8). It is a radial single-phase system with bus 1 as a substation bus or reference bus. In a traditional radial system, the substation bus is the only bus that has generation units on it and is assumed to be infinite capacity. The detailed power-flow results for the IEEE 33bw-bus system using HELM are mentioned in Appendix B. In Figure (9), it can be noted that for more than 15 terms in the power series, there is no significant reduction in mismatch error for the case.

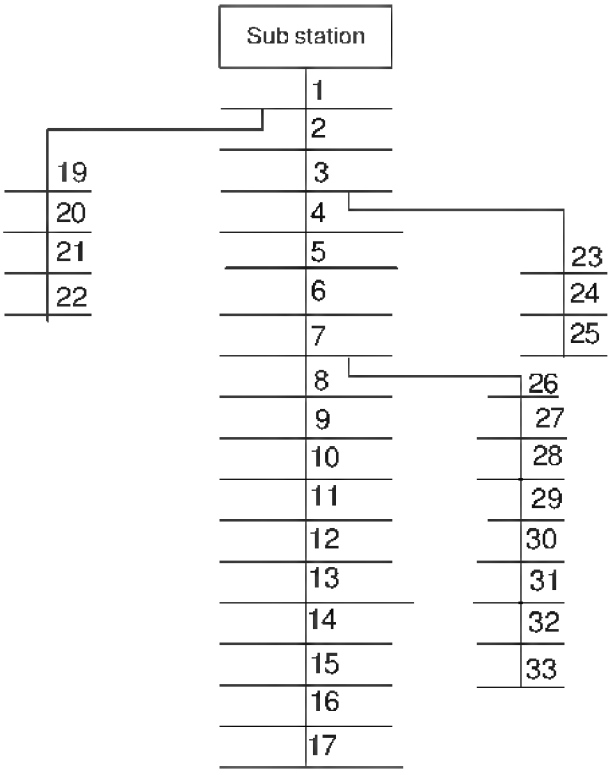

Figure 8 – Single Line Diagram of IEEE 33bw-bus case

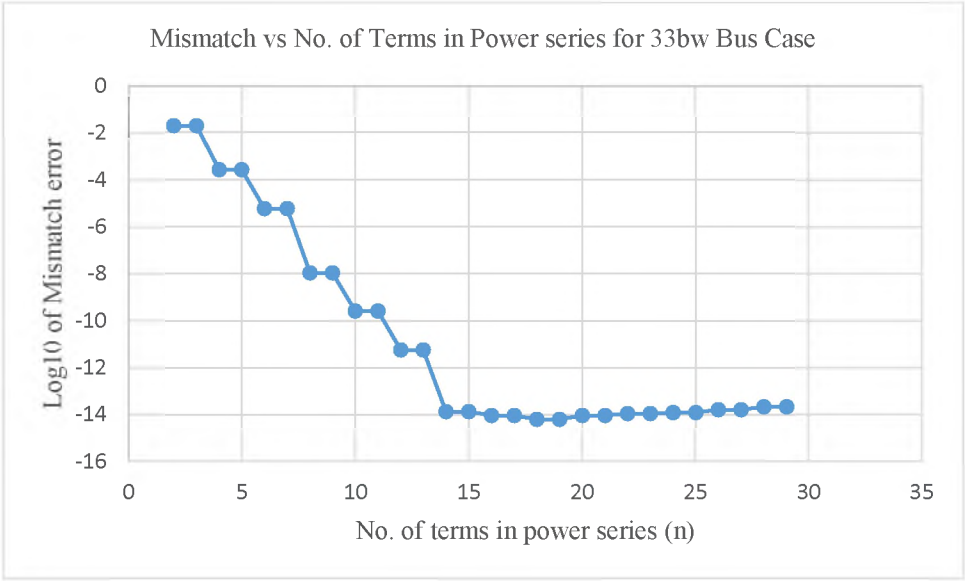

Figure 9 - Highest Absolute Mismatch of PBE vs Number of terms in Power series for IEEE 33bw-Bus Case

4.2.1.3 IEEE 118-bus system

Figure (10) represents IEEE 118-bus system on which HELM was also applied. Figure (11) represents the relationship between mismatch error and the number of terms in the power series of voltage in PBEs. With the increase in the number of terms in the voltage power series, the mismatch error decreases; however, the decrease is not monotonic, but oscillating in nature. It can be noted that the mismatch becomes nearly constant for values of $n > 18$. The full results of load-flow results using HELM can be found in Appendix C.

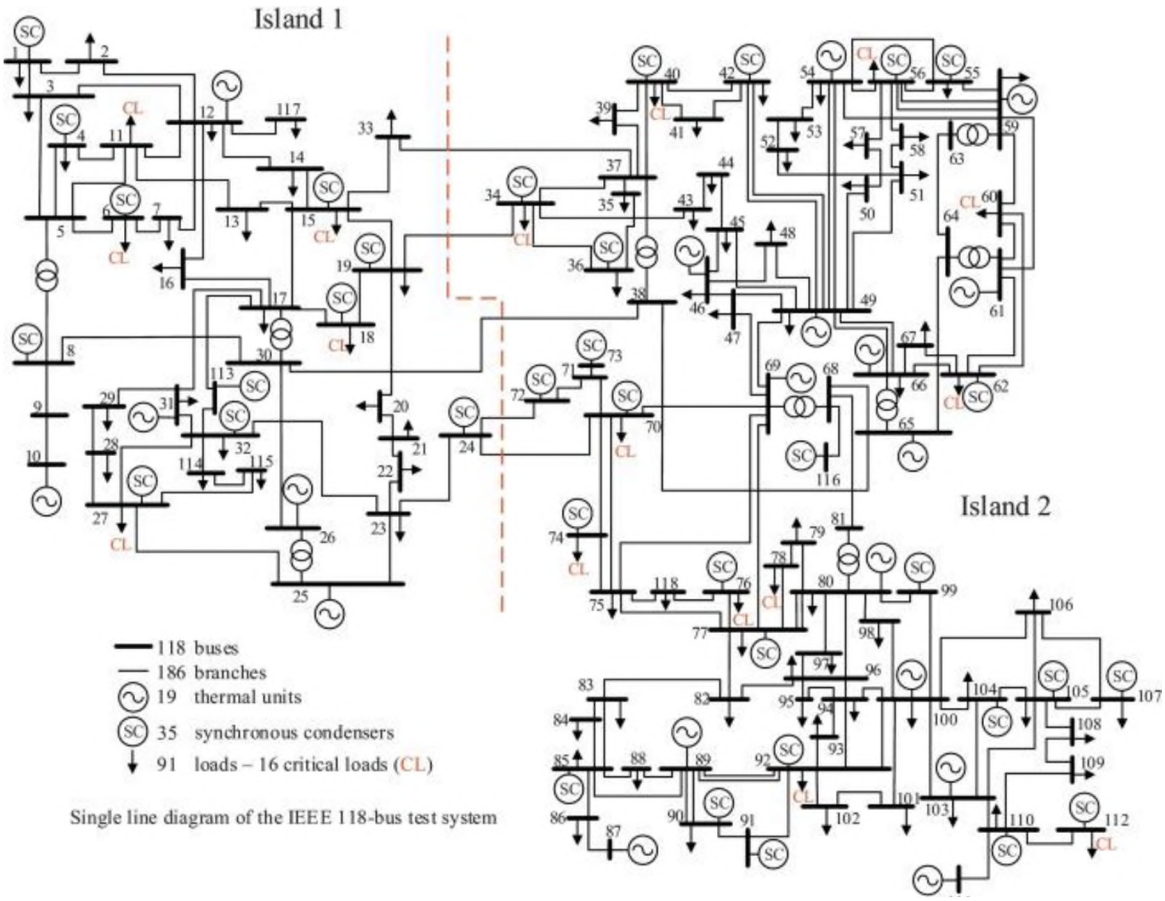

Figure 10 - Single Line Diagram of IEEE 118-Bus Case

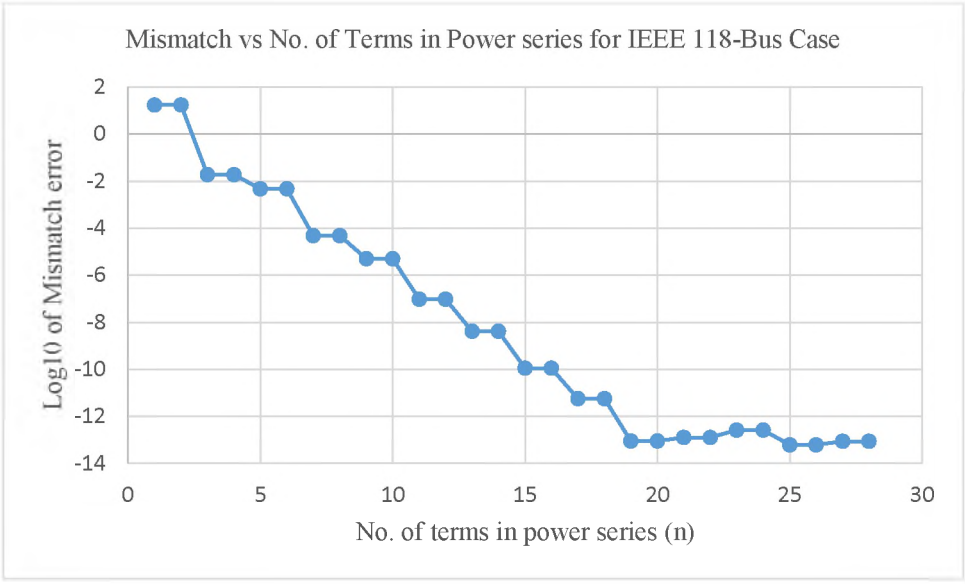

Figure 11 - Highest Absolute Mismatch of PBE vs Number of terms in Power series for IEEE 118-Bus Case

4.2.1.4 IEEE 300-bus system

Figure (13) represents IEEE 300-bus system on which HELM was applied. Figure (12) represents a relationship between mismatch error and the number of terms in the power series of voltage in PBEs. Again, with the increase in the number of terms in power series, the mismatch error decreases; however, the decrease is not monotonic, but oscillating in nature. It can be noted that the mismatch becomes nearly constant for values of $n > 44$. The summary of load-flow results using HELM results is below:

Total Mw Generated = 23935.376	Total MVar Generated = 7983.709
Total Mw Load = 23525.85	Total MVar Load = 7787.97
Total Mw Loss = 409.526	Total MVar Loss = 195.739
Mw Shunt Losses: -0.214	MVar Shunt Losses: -599.525

	Maximum:	Minimum:
Voltage Mag:	1.0734999999999981	0.9287992618042102
Voltage Ang:	35.07237077770962	-37.54254862965541

Coefficients in Voltage series = 40	Number of Buses = 300
Convergence Status = true	Number of Branches = 411
Initial condition = Flat Start	Mismatch Value = 1.6566e-12

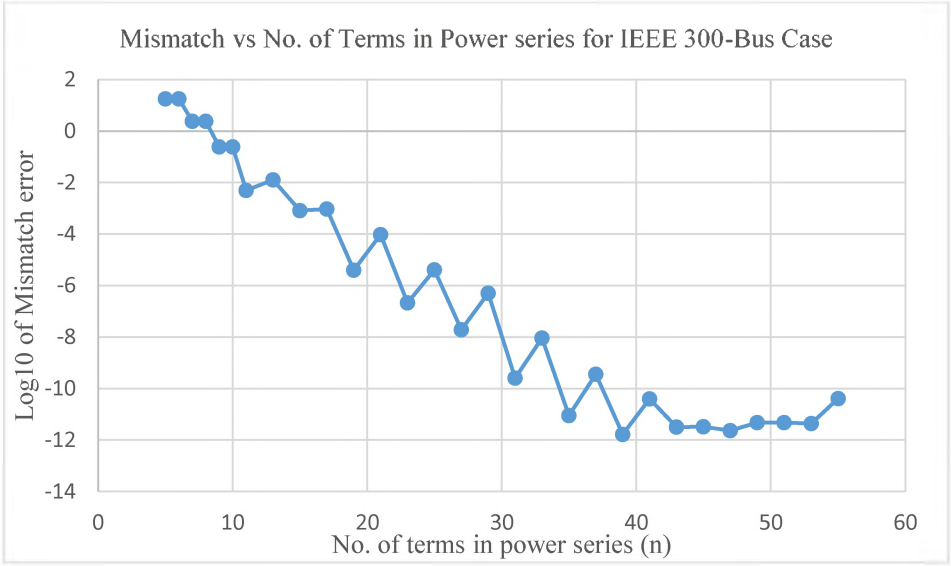

Figure 12 - Highest Absolute Mismatch of PBE vs Number of terms in Power series for IEEE 300-Bus Case

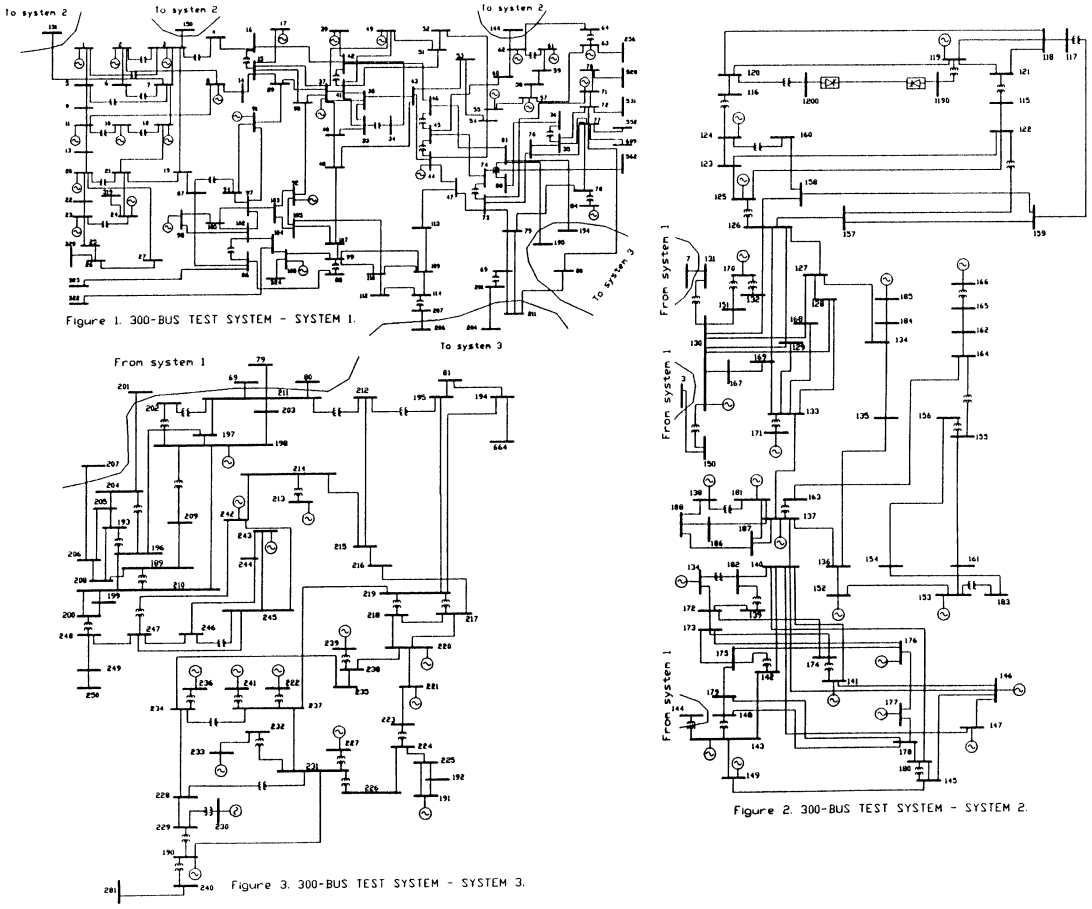

Figure 13 - Single Line Diagram of IEEE 300-Bus Case

4.2.2 Three-phase bus system

The three-phase modeling is accurate than a single-phase modeling of a power system. It has advantages such as the inclusion of mutual impedance in the admittance matrix. In a single-bus equivalent system, the off-diagonal elements of a phase-frame matrix, like one in the equation (2.13), are zero and all the diagonal element has the same value. This reduces the complexity and eases computational time but increases in accuracy. Therefore, the HELM is applied to the distribution system for detailed application.

4.2.2.1 IEEE 37-bus three-phase feeder/system

Figure (16) shows the IEEE 37-bus system is shown in Appendix D. The substation is connected to Bus 799 which is also called reference bus for the system. The IEEE 37-bus system is an unbalanced radial distribution system with a total of 111 phase-nodes and a total of 37 bus. The reference bus has a nominal voltage with a positive phase sequence. Figure (14) maps the relation between mismatch error and the number of terms in power series. It can be noted that after 25 terms, in the holomorphically embedded voltage power series, the mismatch remains constant. Therefore, using such knowledge computational time can be optimized for the IEEE 37-bus system.

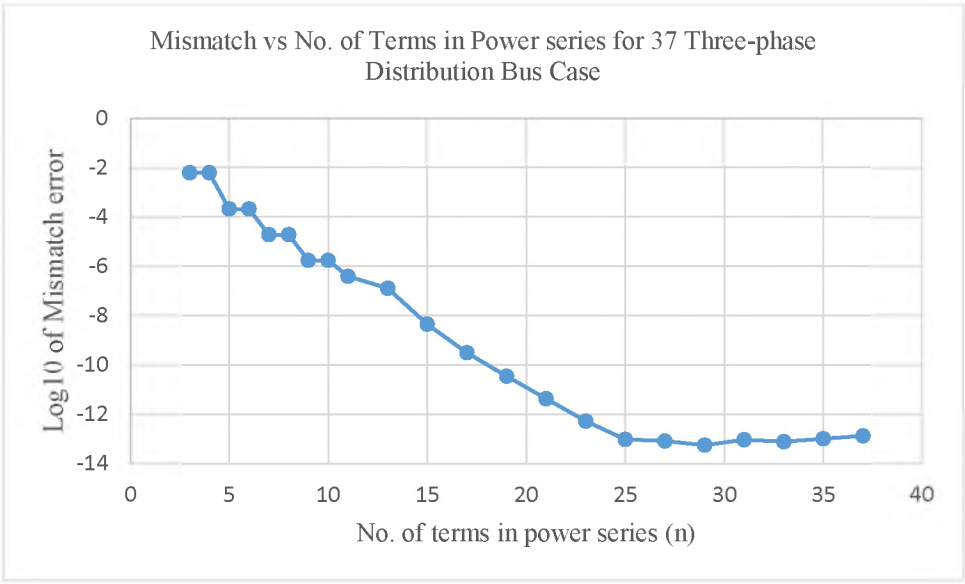

Figure 14 - Highest Absolute Mismatch of PBE vs Number of terms in Power series for IEEE 37-Bus Case

From Table (4), it can be analytically noted that the quality of voltage magnitude and angle on each node deviates from ideal as we go from substation node to downward nodes. One solution to improving the voltage profile on nodes that are further from the substation is to use a voltage regulating transformer.

Table 4 - Power-Flow Solution for Each Phase of IEEE 37-Bus Case

Bus id	Phase A		Phase B		Phase C	
	Voltage Magnitude (p.u.)	Voltage Angle (Degree)	Voltage Magnitude (p.u.)	Voltage Angle (Degree)	Voltage Magnitude (p.u.)	Voltage Angle (Degree)
799 (Ref. bus)	1.000	0.000	1.000	-120.000	1.000	120.000
701	0.995	-0.701	0.999	-120.480	0.992	118.961
702	0.992	-1.142	0.997	-120.741	0.989	118.439
703	0.988	-1.687	0.998	-120.861	0.986	118.047
704	0.990	-1.161	0.993	-121.052	0.989	118.245
705	0.992	-1.128	0.996	-120.796	0.988	118.351
706	0.990	-1.014	0.987	-121.363	0.990	118.058
707	0.989	-0.890	0.980	-121.738	0.991	117.997
708	0.982	-2.425	1.000	-120.827	0.977	117.604
709	0.984	-2.201	0.999	-120.859	0.979	117.701
710	0.979	-2.935	1.000	-120.776	0.969	117.252
711	0.975	-3.414	1.004	-120.651	0.965	117.186
712	0.992	-1.131	0.996	-120.778	0.987	118.299
713	0.991	-1.154	0.995	-120.854	0.989	118.326
714	0.990	-1.180	0.993	-121.058	0.989	118.252
718	0.988	-1.293	0.993	-121.063	0.989	118.287
720	0.990	-1.034	0.988	-121.316	0.989	118.062
722	0.989	-0.876	0.980	-121.780	0.992	117.989
724	0.989	-0.862	0.979	-121.822	0.992	117.994
725	0.990	-1.003	0.987	-121.394	0.990	118.057
727	0.986	-1.761	0.998	-120.872	0.985	118.017
728	0.985	-1.838	0.998	-120.905	0.984	118.004
729	0.985	-1.853	0.999	-120.891	0.985	118.029
730	0.985	-2.075	0.999	-120.849	0.980	117.764
731	0.984	-2.160	0.998	-120.949	0.980	117.693
732	0.982	-2.427	1.000	-120.815	0.976	117.567
733	0.980	-2.646	1.001	-120.806	0.974	117.532
734	0.978	-2.946	1.002	-120.760	0.971	117.370
735	0.979	-2.938	1.000	-120.761	0.968	117.207
736	0.979	-2.890	0.998	-120.912	0.970	117.248
737	0.975	-3.295	1.004	-120.725	0.968	117.345
738	0.975	-3.404	1.004	-120.693	0.967	117.285
740	0.976	-3.417	1.004	-120.636	0.965	117.141
741	0.976	-3.418	1.004	-120.637	0.965	117.152
742	0.991	-1.111	0.995	-120.863	0.989	118.351
744	0.986	-1.822	0.999	-120.890	0.985	118.020
775	0.984	-2.201	0.999	-120.859	0.979	117.701

Figure (15) shows the graphical variation of voltage magnitude and voltage angle on each phase node of the IEEE 37-bus system. It is interesting to note the decline of voltage magnitude for buses that are further away from substation bus due to voltage drop on each previous bus on the current path. Figure (15) also gives an insight on strategic bus locations on which distributed energy resources, such as photovoltaic panels, battery bank or other power quality correction methods, can be installed for improved voltage profile. For example, a voltage correction method could be installed at bus 13 so that it can improve the voltage in that neighborhood.

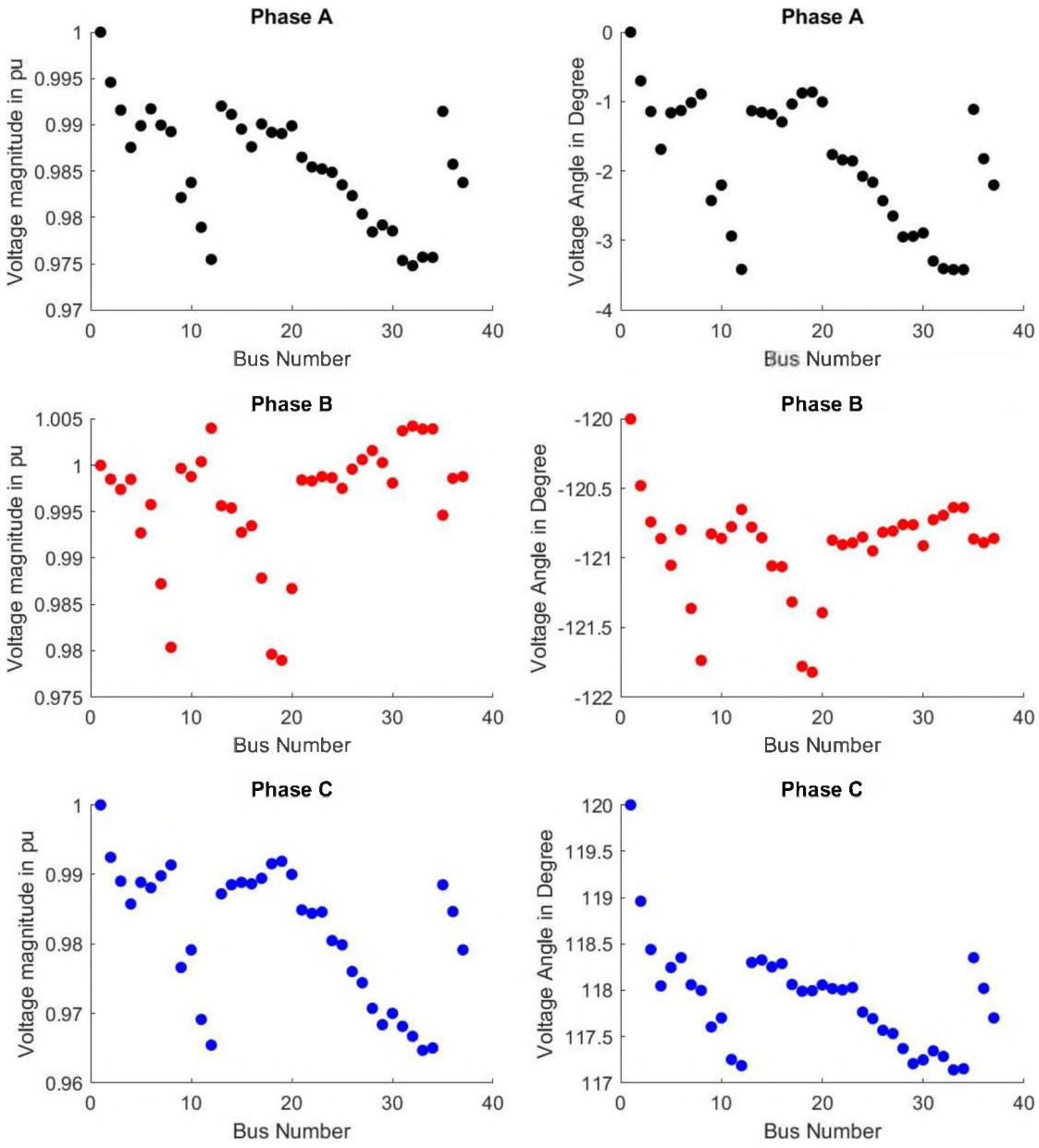

Figure 15 – Phase-wise Voltage Magnitude and Angle for IEEE 37-Bus Case

4.3 Performance Summary

To understand the performance of HELM on various IEEE bus systems, average time performance using Benchmarking package in Julia environment was used. In Table (5), the number of power series coefficients for each bus is $n = 50$. The value of n can be decreased or increased to improve the performance as a minimum number of coefficients reduces the computational cost. However, for case-wise comparison, the number of coefficients are chosen to be 50. From Table (5), it is clear to note that as the number of buses in a case system increases, the average time taken to execute the algorithm is increased.

Table 5 - Time Performance Comparison of HELM using Benchmarking Tool Package in Julia

Case Name	Tap Changer Transformer	Number of Samples	Total Mean Run Time (Milliseconds)
case5	N	158	31.687 ms
case9	N	122	41.101 ms
case14	Y	85	58.829 ms
case30	N	39	128.145 ms
case57	Y	25	202.941 ms
case89pegase	Y	13	400.120 ms
case118	Y	9	574.574 ms
case300	Y	3	1692 ms
case1354pegase	Y	1	7275 ms
case9241pegase	Y	1	952549 ms

4.4 Advantages and Disadvantages of HELM

The advantages of HELM solve many of the issues of traditional power flow methods. HELM provides voltage solution on the higher voltage side of the PV curve, if it exists, and numerically expresses if the solution does not exist.

CHAPTER V

CONCLUSION & FUTURE SCOPE

5.1 Conclusion

The research presented here implemented HELM on various single-phase networks and three-phase unbalanced networks. The details of Holomorphic load flow modeling for a different type of loads were discussed. Theoretically, a voltage power series can have an infinite number of terms and for infinite computing precision, HELM guarantees the high-voltage operable solution, if it exists. It was observed that to obtain a solution for different networks, with finite set error, a different number of terms in the holomorphically embedded voltage power series shall be selected for better performance. The performance and accuracy of distributed power flow methods like the ladder-iterative method are shown to be slower than HELM. It is also observed that net power injection mismatch error reduces almost quadratically, however, the error decreases non-monotonically with an increase in the number of terms in power series. Further, it was also noted that the most time-consuming step was the calculation of Pade` approximant, due to its complexity of $O(M^3)$.

5.2 Future Scope

The HELM seems very promising for various power flow and its derivative applications, such as Economic Dispatch and Optimal Power Flow, with both AC and DC assumptions [37]. Although the iterative techniques for power-flow studies, like Newton Raphson (NR), do not require an additional step of calculating Pade` approximant, which takes additional calculation resources. However, this is countered by the requirement of calculating the Jacobian matrix for each iteration in the NR method. To further improve the speed of the HELM, the analytic continuation (Pade` approximant) step can be performed in parallel on all the buses as there is no relating factor between voltage series of buses.

For further improvement of the Algorithm's performance, LU factorization can be employed and a better starting point, aka Germ solution, can be determined. The starting point of HELM can be the second or third iteration result of methods like the Gauss-Seidel power flow method, this is theorized to improve the performance to large extent [7], [24]. Further, the robustness of HELM can be investigated especially for synthetic cases and systems with islanding, which can occur in very large power systems. The Algorithm can further be extended to Delta-connected ZIP load and other three-phase components like the voltage regulator and various winding configurations of a three-phase transformer.

REFERENCES

[1] J. D. Glover, M. S. Sarma and T. J. Overbye, "Power System Analysis and Design 4th Edition," Cengage Learning, Stamford, 2007.

[2] B. Stott, "Review of Load-Flow Calculation Methods," in *PROCEFSMGS of the IEEE*, vol. 62, No. 7, pp. 916-929, Jul. 1974.

[3] W. Tinney and C. Hart, "Power flow solution by Newton's method," in *IEEE Transactions Power Application System*, vol. PAS-86, no. 11, pp. 1449-1460, Nov. 1967.

[4] A. Trias, "The Holomorphic Embedding Load Flow Method," in *IEEE PES General Meeting*, San Diego, CA, July 2012, pp. 1-8.

[5] V. Ajjarapu and C. Christy, "The continuation power flow: a tool for steady state voltage stability analysis," [Proceedings] Conference Papers 1991 Power Industry Computer Application Conference, Baltimore, MD, USA, 1991, pp. 304-311, doi: 10.1109/PICA.1991.160593.

[6] Antonio Trias and J. L. Marín, "The Holomorphic Embedding Load flow Method for DC Power Systems and Nonlinear DC Circuits," in *IEEE Transactions on Circuits and Systems I: Regular Papers*, vol. 63, no. 2, pp. 322-333, Feb. 2016.

[7] W. H. Kersting, "Distribution System Modeling and Analysis: Fourth Edition," CRC Press, 2018.

[8] J.-H. Teng, "A direct approach for distribution system load-flow solutions," in *IEEE Transactions on Power Delivery*, vol. 18, no. 3, pp. 882–887, July 2003.

[9] S. Petridis, O. Blanas, D. Rakopoulos, F. Stergiopoulos, N. Nikolopoulos, and S. Voutetakis, "An Efficient Backward/Forward Sweep Algorithm for Power Flow

Analysis through a Novel Tree-Like Structure for Unbalanced Distribution Networks," in *Energies*, vol. 14, no. 4, p. 897, Feb. 2021.

[10] Bazrafshan, and Nikolaos Gatsis, "Comprehensive Modeling of Three-Phase Distribution Systems via the Bus Admittance Matrix," in *IEEE Transactions on Power Systems*, Vol: 33, Issue: 2, March 2018.

[11] R. D. Zimmerman, C. E. Murillo-Sanchez, and R. J. Thomas, "MATPOWER: Steady-State Operations, Planning and Analysis Tools for Power Systems Research and Education," *Power Systems*, *IEEE Transactions* on, vol. 26, no. 1, pp. 12–19, Feb. 2011.

[12] R. D. Zimmerman, C. E. Murillo-Sanchez (2020). MATPOWER (Version 7.1) [Software]. Available: https://matpower.org

[13] R. D. Zimmerman, C. E. Murillo-Sanchez. MATPOWER User's Manual. 2020. [Online]. Available: https://matpower.org/docs/MATPOWER-manual.pdf

[14] K. P. Schneider et al., "Analytic Considerations and Design Basis for the IEEE Distribution Test Feeders," in *IEEE Transactions on Power Systems*, vol. PP, no. 99, pp. 1-1, 2017.

[15] H. C. Chen, L. Y. Chung, "Load Flow Solution for ill-conditioned by Homotopy Continuation Method," in *International Journal of Power and Energy Systems*, Vol. 28, No. 1, pp. 99-105, 2008.

[16] J. Thorp and S. Naqavi, "Load-flow fractals draw clues to erratic behavior," in *IEEE Computer Application Power*, vol. 10, no. 1, pp. 59-62, Jan. 1997.

[17] Carson, J. R., "Wave propagation in overhead wires with ground return," in *Bell System Technical Journal*, Vol. 5, pp. 539–554, 1926.

[18] Kron, G., "Tensorial analysis of integrated transmission systems, part I, the six basic reference frames," in *Transactions of the American Institute of Electrical Engineers*, Vol. 71, pp. 814–882, 1952.

[19] H. Stahl, "On the convergence of generalized Padé approximants," Constructive Approximation, vol. 5, pp. 221–240, 1989.

[20] Diego Issicaba, Jorge Coelho, "Evaluation of the Forward-Backward Sweep Load Flow Method using the Contraction Mapping Principle," in *International Journal of Electrical and Computer Engineering,* Vol. 6, No. 6.

[21] D. J. Tylavsky, P. E. Crouch, L. F. Jarriel, and H. Chen, "Advances in Fast Power Flow Algorithms," in *Advances in Theory and Applications, Control and Dynamics*, Volume 42, Part 4 of 4, pp. 295-344, Academic Press, 1991.

[22] Xu, W., Y. Liu, J. Salmon, T. Le, and G. Chang. 1998. "Series load flow: a novel noniterative load flow method". *Generation, Transmission and Distribution, IEE Proceedings*-. 145(3): 251–256. ISSN: 1350-2360. DOI: 10.1049/ip-gtd:19981980.

[23] C. Liu, K. Sun, B. Wang and W. Ju, "Probabilistic Power Flow Analysis Using Multidimensional Holomorphic Embedding and Generalized Cumulants," in *IEEE Transactions on Power Systems*, vol. 33, no. 6, pp. 7132-7142, Nov. 2018.

[24] G. Baker, P. Graves-Morris, "Padé approximants", *Series: Encyclopedia of Mathematics and its applications*, Cambridge University Press, 1996.

[25] S. Rao, Y. Feng, D. J. Tylavsky and M. K. Subramanian, "The Holomorphic Embedding Method Applied to the Power-Flow Problem," in *IEEE Transactions on Power Systems*, vol. 31, no. 5, pp. 3816-3828, Sept. 2016, doi: 10.1109/TPWRS.2015.2503423.

[26] M. Subramanian, Y. Feng and D. Tylavsky, "PV Bus Modeling in a Holomorphically Embedded Power-Flow Formulation," in *North American Power Symposium,* Sep. 2013, pp. 1-6.

[27] J. Nuttall, "On convergence of Padé approximants to functions with branch points" in *Padé and Rational Approximation*, New York, NY USA: Academic, pp. 101-109, 1977.

[28] P. Henrici, Applied and Computational Complex Analysis. Vol. 3: Discrete Fourier Analysis Cauchy Integrals Construction of Conformal Maps Univalent Functions, New York, NY USA: Wiley, 1986.

[29] Li, Yuting, Tylavsky, Daniel, et al., "Effect of Various Holomorphic Embeddings on Convergence Rate and Condition Number as Applied to the Power Flow Problem," *Thesis Presented in Partial Fulfillment of the Requirements for the Degree Master of Science*, pp. 50, Arizona State University, 2015.

[30] L. Sun, Y. Ju, L. Yang, S. Ge, Q. Fang and J. Wang., "Holomorphic Embedding Load Flow Modeling of the Three-phase Active Distribution Network," *2018 International Conference on Power System Technology (POWERCON)*, Guangzhou, 2018, pp. 488-495.

[31] C. Liu, B. Wang, F. Hu, K. Sun and C. L. Bak, "Online Voltage Stability Assessment for Load Areas Based on the Holomorphic Embedding Method," in *IEEE Transactions on Power Systems*, vol. 33, no. 4, pp. 3720-3734, July 2018.

[32] Y. Zhu, D. Tylavsky and S. Rao, "Nonlinear Structure-Preserving Network Reduction Using Holomorphic Embedding," in *IEEE Transactions on Power Systems*, vol. 33, no. 2, pp. 1926-1935, March 2018.

[33] B. Wang, C. Liu and K. Sun, "Multi-Stage Holomorphic Embedding Method for Calculating the Power-Voltage Curve," in *IEEE Transactions on Power Systems*, vol. 33, no. 1, pp. 1127-1129, Jan. 2018.

[34] C. Liu, B. Wang, X. Xu, K. Sun, D. Shi and C. L. Bak, "A Multi-Dimensional Holomorphic Embedding Method to Solve AC Power Flows," in *IEEE Access*, vol. 5, pp. 25270-25285, 2017.

[35] Bezanson, Jeff and Edelman, Alan and Karpinski, Stefan and Shah, Viral B, "Julia: A fresh approach to numerical computing," *SIAM review*, vol. 59, no. 1, pp. 65–98, 2017.

[36] IEEE standard Power bus cases. Available at https://icseg.iti.illinois.edu/power-cases/

[37] H. Gao, J. Chen, R. Diao and J. Zhang, "A HEM-Based Sensitivity Analysis Method for Fast Voltage Stability Assessment in Distribution Power Network," in *IEEE Access*, vol. 9, pp. 13344-13353, 2021, doi: 10.1109/ACCESS.2021.3051843.

APPENDIX A

Modified IEEE 5-Bus Case Data

Table 6 - Branch Data for Modified IEEE 5-Bus Case

Branch	Resistance in p.u.	Reactance in p.u.	Shunt susceptance in p.u.
1-2	0.00281	0.0281	0.00712
1-4	0.00304	0.0304	0.00658
1-5	0.00064	0.0064	0.3126
2-3	0.00108	0.0108	0.01852
3-4	0.00	0.43	0
4-5	0.00297	0.0297	0.00674

Table 7 – Bus Injection Data for Modified IEEE 5-Bus Case

Bus Id	Buys Type	Complex Power Generation (MW + j MVAR)	Complex Power load (MW + j MVAR)	Set Voltage in p.u.
1	PV	(40+170) + j 0.0	0.0 + j 0.0	1 ∠0°
2	PQ	•	300 + j 98.61	•
3	PV	323.49 + j 0.0	300 + j 98.61	1 ∠0°
4	REF	0.0 + j 0.0	400 + j 131.47	1 ∠0°
5	PV	466.51 + j 0.0	0.0 + j 0.0	1 ∠0°

APPENDIX B

Results from HELM for IEEE 33bw-bus Single-Phase Case

Table 8 - Power-Flow Solution for IEEE 33bw-Bus Case

Bus Id	Bus Type	Voltage Magnitude (p.u.)	Voltage Angle (Degree)	Net MW Injection	Net MVar Injection
1	REF	1	0	3.91768	2.43514
2	PQ	0.997032	0.014481	-0.1	-0.06
3	PQ	0.982938	0.096042	-0.09	-0.04
4	PQ	0.975456	0.161651	-0.12	-0.08
5	PQ	0.968059	0.228285	-0.06	-0.03
6	PQ	0.949658	0.133853	-0.06	-0.02
7	PQ	0.946173	-0.09647	-0.2	-0.1
8	PQ	0.941328	-0.0604	-0.2	-0.1
9	PQ	0.935059	-0.13348	-0.06	-0.02
10	PQ	0.929244	-0.19601	-0.06	-0.02
11	PQ	0.928384	-0.18876	-0.045	-0.03
12	PQ	0.926885	-0.17727	-0.06	-0.035
13	PQ	0.920772	-0.26859	-0.06	-0.035
14	PQ	0.918505	-0.34727	-0.12	-0.08
15	PQ	0.917093	-0.38495	-0.06	-0.01
16	PQ	0.915725	-0.40821	-0.06	-0.02
17	PQ	0.913698	-0.48547	-0.06	-0.02
18	PQ	0.91309	-0.49506	-0.09	-0.04
19	PQ	0.996504	0.003651	-0.09	-0.04
20	PQ	0.992926	-0.06333	-0.09	-0.04
21	PQ	0.992222	-0.08269	-0.09	-0.04
22	PQ	0.991584	-0.10303	-0.09	-0.04
23	PQ	0.979352	0.06508	-0.09	-0.05
24	PQ	0.972681	-0.02365	-0.42	-0.2
25	PQ	0.969356	-0.06735	-0.42	-0.2
26	PQ	0.947729	0.17331	-0.06	-0.025
27	PQ	0.945165	0.229463	-0.06	-0.025
28	PQ	0.933726	0.312409	-0.06	-0.02
29	PQ	0.925507	0.390314	-0.12	-0.07
30	PQ	0.92195	0.495586	-0.2	-0.6
31	PQ	0.917789	0.411178	-0.15	-0.07
32	PQ	0.916873	0.388135	-0.21	-0.1
33	PQ	0.91659	0.380405	-0.06	-0.04

Total Mw Generated = 3.918 Total MVar Generated = 2.435

Total Mw Load = 3.715 Total MVar Load = 2.3

Total Mw Loss = 0.203	Total MVar Loss = 0.135
Mw Shunt Losses: -0.0	MVar Shunt Losses:0.0
Coefficients in Voltage series = 40	Number of Buses = 33
Convergence Status = true	Number of Branches = 32
Initial condition = Flat Start	Mismatch Value = 7.6319e-15

APPENDIX C

Results from HELM for IEEE 118-bus Single-Phase Case

Table 9 - Power-Flow Solution for IEEE 118-Bus Case

Bus Id	Bus Type	Voltage Magnitude (p.u.)	Voltage Angle (Degree)	Net MW Injection	Net MVar Injection
1	PV	0.955	-19.0273	-51	-30.1041
2	PQ	0.971393	-18.4875	-20	-9
3	PQ	0.967692	-18.1438	-39	-10
4	PV	0.998	-14.4259	-39	-27.0096
5	PQ	1.00198	-13.9808	0	0
6	PV	0.99	-16.7081	-52	-6.07023
7	PQ	0.989328	-17.1527	-19	-2
8	PV	1.015	-8.95942	-28	63.1384
9	PQ	1.04292	-1.70531	0	0
10	PV	1.05	5.8756	450	-51.0422
11	PQ	0.985089	-16.9942	-70	-23
12	PV	0.99	-17.5111	38	81.2917
13	PQ	0.968302	-18.3703	-34	-16
14	PQ	0.983591	-18.2285	-14	-1
15	PV	0.97	-18.5259	-90	-22.8395
16	PQ	0.983897	-17.8127	-25	-10
17	PQ	0.995089	-16.0048	-11	-3
18	PV	0.973	-18.2192	-60	-5.57368
19	PV	0.962	-18.6854	-45	-39.2742
20	PQ	0.956934	-17.809	-18	-3
21	PQ	0.957725	-16.222	-14	-8
22	PQ	0.969019	-13.6684	-10	-5
23	PQ	0.999469	-8.7513	-7	-3
24	PV	0.992	-8.88613	-13	-14.9076
25	PV	1.05	-1.82016	220	50.0433
26	PV	1.015	-0.0398	314	10.1247
27	PV	0.968	-14.3956	-71	-9.01765
28	PQ	0.961568	-16.1211	-17	-7
29	PQ	0.963216	-17.1146	-24	-4
30	PQ	0.985333	-10.9662	0	0
31	PV	0.967	-16.9981	-36	5.58601
32	PV	0.963	-14.9394	-59	-39.2848
33	PQ	0.970934	-19.1462	-23	-9
34	PV	0.984	-18.4886	-59	-46.8271

35	PQ	0.980452	-18.9449	-33	-9
36	PV	0.98	-18.9445	-31	-9.27492
37	PQ	0.990661	-18.0333	0	0
38	PQ	0.961286	-12.8924	0	0
39	PQ	0.969961	-21.4234	-27	-11
40	PV	0.97	-22.5045	-66	5.45407
41	PQ	0.966832	-22.9484	-37	-10
42	PV	0.985	-21.3471	-96	18.0296
43	PQ	0.977121	-18.5396	-18	-7
44	PQ	0.984436	-16.0567	-16	-8
45	PQ	0.986383	-14.2274	-53	-22
46	PV	1.005	-11.4243	-9	-15.0295
47	PQ	1.01705	-9.20087	-34	-1.79E-12
48	PQ	1.02063	-9.9815	-20	-11
49	PV	1.025	-8.97839	117	85.8451
50	PQ	1.00108	-11.0171	-17	-4
51	PQ	0.966877	-13.6358	-17	-8
52	PQ	0.956818	-14.5891	-18	-5
53	PQ	0.945983	-15.5639	-23	-11
54	PV	0.955	-14.6519	-65	-28.0989
55	PV	0.952	-14.9418	-63	-17.3358
56	PV	0.954	-14.7551	-84	-20.2857
57	PQ	0.970583	-13.5508	-12	-3
58	PQ	0.959039	-14.4075	-12	-3
59	PV	0.985	-10.5515	-122	-36.166
60	PQ	0.993156	-6.76988	-78	-3
61	PV	0.995	-5.87851	160	-40.394
62	PV	0.998	-6.49517	-77	-12.7416
63	PQ	0.968737	-7.17259	0	0
64	PQ	0.983739	-5.40664	0	0
65	PV	1.005	-2.2809	391	81.5102
66	PV	1.05	-2.44132	353	-19.9566
67	PQ	1.01968	-5.08103	-28	-7
68	PQ	1.00325	-2.40217	0	0
69	REF	1.035	0	513.863	-82.4241
70	PV	0.984	-7.38208	-66	-10.3307
71	PQ	0.986845	-7.7931	0	0
72	PV	0.98	-8.89144	-12	-11.1301
73	PV	0.991	-8.00459	-6	9.65137
74	PV	0.958	-8.33144	-68	-32.6252
75	PQ	0.967332	-7.06979	-47	-11
76	PV	0.943	-8.20121	-68	-30.7319
77	PV	1.006	-3.24936	-61	-15.8296

78	PQ	1.00342	-3.55339	-71	-26
79	PQ	1.00922	-3.25456	-39	-32
80	PV	1.04	-1.00993	347	79.4665
81	PQ	0.996807	-1.85511	0	0
82	PQ	0.988545	-2.72826	-54	-27
83	PQ	0.984377	-1.53605	-20	-10
84	PQ	0.979704	1.00031	-11	-7
85	PV	0.985	2.55562	-24	-20.6066
86	PQ	0.986691	1.18617	-21	-10
87	PV	1.015	1.44539	4	11.0216
88	PQ	0.987453	5.69035	-48	-10
89	PV	1.005	9.74834	607	-5.90495
90	PV	0.985	3.33837	-163	17.3084
91	PV	0.98	3.35064	-10	-13.088
92	PV	0.99	3.8808	-65	-23.9562
93	PQ	0.985433	0.849095	-12	-7
94	PQ	0.98983	-1.31779	-30	-16
95	PQ	0.980332	-2.29044	-42	-31
96	PQ	0.992283	-2.45741	-38	-15
97	PQ	1.01117	-2.08416	-15	-9
98	PQ	1.02351	-2.56665	-34	-8
99	PV	1.01	-2.93323	-42	-17.5356
100	PV	1.017	-1.94116	215	77.5521
101	PQ	0.99142	-0.35312	-22	-15
102	PQ	0.989131	2.36499	-5	-3
103	PV	1.01	-5.68225	17	59.4224
104	PV	0.971	-8.25223	-38	-22.6117
105	PV	0.965	-9.35643	-31	-44.3345
106	PQ	0.961146	-9.6166	-43	-16
107	PV	0.952	-12.4173	-50	-5.44218
108	PQ	0.966212	-10.5565	-2	-1
109	PQ	0.967026	-11.0091	-8	-3
110	PV	0.973	-11.856	-39	-29.7192
111	PV	0.98	-10.2109	36	-1.84382
112	PV	0.975	-14.9552	-68	28.5117
113	PV	0.993	-16.0074	-6	6.75263
114	PQ	0.960093	-15.2736	-8	-3
115	PQ	0.960023	-15.2819	-22	-7
116	PV	1.005	-2.83716	-184	51.3225
117	PQ	0.973824	-19.0521	-20	-8
118	PQ	0.949438	-8.05813	-33	-15

Total Mw Generated = 4374.863

Total MVar Generated = 795.684

Total Mw Load = 4242.0

Total MVar Load = 1438.0

Total Mw Loss = 132.863

Total MVar Loss = -642.316

Mw Shunt Losses: -0.0

MVar Shunt Losses:84.41194499999997

Coefficients in Voltage series = 40

Number of Buses = 118

Convergence Status = true

Number of Branches = 186

Initial condition = Flat Start

Mismatch Value = 1.99647132040731e-13

APPENDIX D

Modified IEEE 37-bus Three-Phase Feeder Data

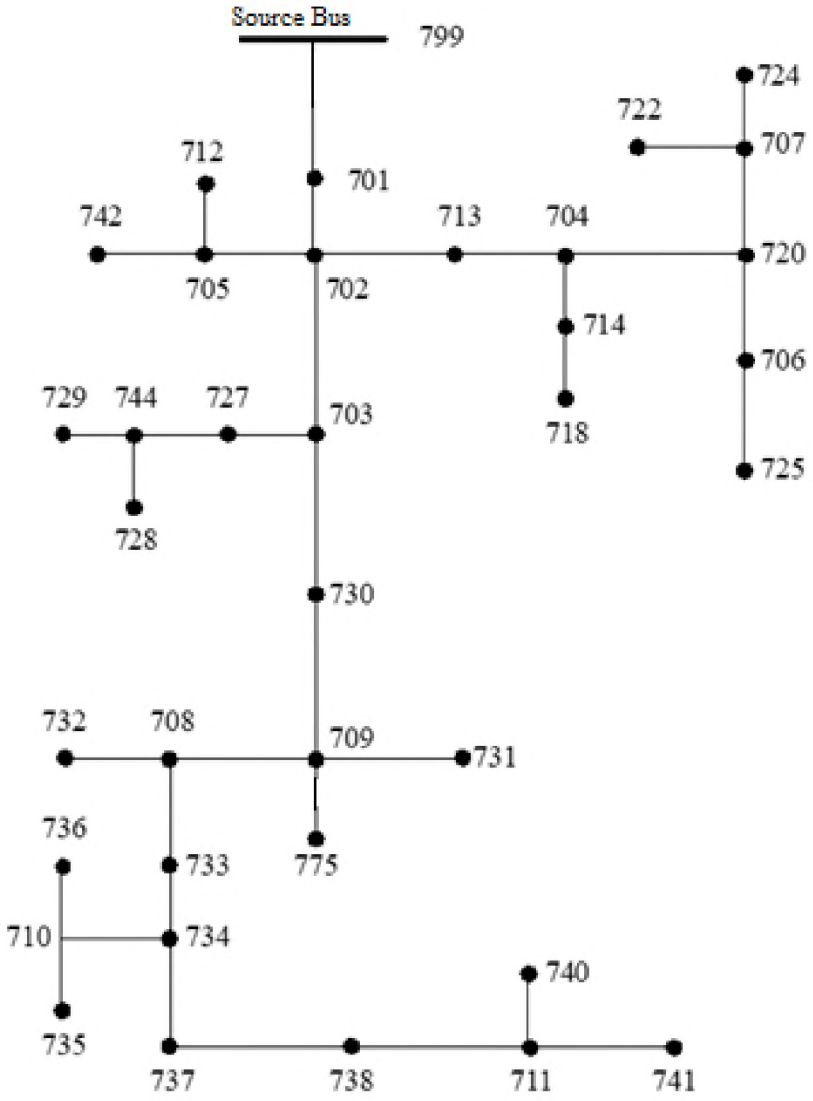

Figure 16 – Single Line Diagram of IEEE 37 Bus Case

Table 10 – Spot Load Data for Modified IEEE 37-Bus Case

Spot Loads							
Node	Load Model	Ph-1 kW	Ph-1 kVAr	Ph-2 kW	Ph-2 kVAr	Ph-3 kW	Ph-4 kVAr
701	Y-PQ	140	70	140	70	350	175
712	Y-PQ	0	0	0	0	85	40
713	Y-PQ	0	0	0	0	85	40
714	Y-PQ	17	8	21	10	0	0
718	Y-PQ	85	40	0	0	0	0
720	Y-PQ	0	0	0	0	85	40
722	Y-PQ	0	0	140	70	21	10
724	Y-PQ	0	0	42	21	0	0
725	Y-PQ	0	0	42	21	0	0
727	Y-PQ	0	0	0	0	42	21
728	Y-PQ	42	21	42	21	42	21
729	Y-PQ	42	21	0	0	0	0
730	Y-PQ	0	0	0	0	85	40
731	Y-PQ	0	0	85	40	0	0
732	Y-PQ	0	0	0	0	42	21
733	Y-PQ	85	40	0	0	0	0
734	Y-PQ	0	0	0	0	42	21
735	Y-PQ	0	0	0	0	85	40
736	Y-PQ	0	0	42	21	0	0
737	Y-PQ	140	70	0	0	0	0
738	Y-PQ	126	62	0	0	0	0
740	Y-PQ	0	0	0	0	85	40
741	Y-PQ	0	0	0	0	42	21
742	Y-PQ	8	4	85	40	0	0
744	Y-PQ	42	21	0	0	0	0
Total		727	357	639	314	1091	530

Table 11 – Branch Data for Modified IEEE 37-Bus Case

Line Segment Data			
Node A	Node B	Length(ft.)	Config.
701	702	960	722
702	705	400	724
702	713	360	723
702	703	1320	722
703	727	240	724
703	730	600	723
704	714	80	724
704	720	800	723
705	742	320	724
705	712	240	724
706	725	280	724
707	724	760	724
707	722	120	724
708	733	320	723
708	732	320	724
709	731	600	723
709	708	320	723
710	735	200	724
710	736	1280	724
711	741	400	723
711	740	200	724
713	704	520	723
714	718	520	724
720	707	920	724
720	706	600	723
727	744	280	723
730	709	200	723
733	734	560	723
734	737	640	723
734	710	520	724
737	738	400	723
738	711	400	723
744	728	200	724
744	729	280	724
775	709	100	724
799	701	1850	721

Phase Impedance and Admittance Matrices

Configuration 721

$Z = R + jX$ in ohms per mile

0.2926 + j 0.1973 0.0673 - j 0.0368 0.0337 - j 0.0417
0.2646 + j 0.1900 0.0673 - j 0.0368
0.2926 + j 0.1973

jB in micro-Siemens per mile
159.7919 0.0000 0.0000
159.7919 0.0000
159.7919

Configuration 722

$Z = R + jX$ in ohms per mile
0.4751 + j 0.2973 0.1629 - j 0.0326 0.1234 - j 0.0607
0.4488 + j 0.2678 0.1629 - j 0.0326
0.4751 + j 0.2973

jB in micro-Siemens per mile
127.8306 0.0000 0.0000
127.8306 0.0000
127.8306

Configuration 723

$Z = R + jX$ in ohms per mile
1.2936 + j 0.6713 0.4871 + j 0.2111 0.4585 + j 0.1521
1.3022 + j 0.6326 0.4871 + j 0.2111
1.2936 + j 0.6713

jB in micro-Siemens per mile
74.8405 0.0000 0.0000
74.8405 0.0000
74.8405

Configuration 724

$Z = R + jX$ in ohms per mile
2.0952 + j 0.7758 0.5204 + j 0.2738 0.4926 + j 0.2123
2.1068 + j 0.7398 0.5204 + j 0.2738
2.0952 + j 0.7758

jB in micro-Siemens per mile
60.2483 0.0000 0.0000
60.2483 0.0000
60.2483

APPENDIX E

Detailed results from HELM for Modified IEEE 37-bus Three-Phase Feeder

Table 12 - Power-Flow Solution for IEEE 37-Bus Case

Bus id	Phase A		Phase B		Phase C	
	Voltage Magnitude (p.u.)	Voltage Angle (Degree)	Voltage Magnitude (p.u.)	Voltage Angle (Degree)	Voltage Magnitude (p.u.)	Voltage Angle (Degree)
799	1.000	0.000	1.000	-120.000	1.000	120.000
701	0.995	-0.701	0.999	-120.480	0.992	118.961
702	0.992	-1.142	0.997	-120.741	0.989	118.439
703	0.988	-1.687	0.998	-120.861	0.986	118.047
704	0.990	-1.161	0.993	-121.052	0.989	118.245
705	0.992	-1.128	0.996	-120.796	0.988	118.351
706	0.990	-1.014	0.987	-121.363	0.990	118.058
707	0.989	-0.890	0.980	-121.738	0.991	117.997
708	0.982	-2.425	1.000	-120.827	0.977	117.604
709	0.984	-2.201	0.999	-120.859	0.979	117.701
710	0.979	-2.935	1.000	-120.776	0.969	117.252
711	0.975	-3.414	1.004	-120.651	0.965	117.186
712	0.992	-1.131	0.996	-120.778	0.987	118.299
713	0.991	-1.154	0.995	-120.854	0.989	118.326
714	0.990	-1.180	0.993	-121.058	0.989	118.252
718	0.988	-1.293	0.993	-121.063	0.989	118.287
720	0.990	-1.034	0.988	-121.316	0.989	118.062
722	0.989	-0.876	0.980	-121.780	0.992	117.989
724	0.989	-0.862	0.979	-121.822	0.992	117.994
725	0.990	-1.003	0.987	-121.394	0.990	118.057
727	0.986	-1.761	0.998	-120.872	0.985	118.017
728	0.985	-1.838	0.998	-120.905	0.984	118.004
729	0.985	-1.853	0.999	-120.891	0.985	118.029
730	0.985	-2.075	0.999	-120.849	0.980	117.764
731	0.984	-2.160	0.998	-120.949	0.980	117.693
732	0.982	-2.427	1.000	-120.815	0.976	117.567
733	0.980	-2.646	1.001	-120.806	0.974	117.532
734	0.978	-2.946	1.002	-120.760	0.971	117.370
735	0.979	-2.938	1.000	-120.761	0.968	117.207
736	0.979	-2.890	0.998	-120.912	0.970	117.248
737	0.975	-3.295	1.004	-120.725	0.968	117.345
738	0.975	-3.404	1.004	-120.693	0.967	117.285
740	0.976	-3.417	1.004	-120.636	0.965	117.141
741	0.976	-3.418	1.004	-120.637	0.965	117.152
742	0.991	-1.111	0.995	-120.863	0.989	118.351
744	0.986	-1.822	0.999	-120.890	0.985	118.020
775	0.984	-2.201	0.999	-120.859	0.979	117.701